Published OnlineFirst January 10, 2011; DOI: 10.1158/1078-0432.CCR-10-1993

on a FACSCalibur flow cytometer with CellQuest Software (Becton Dickinson).

Statistical analysis

Two-tailed Student's *t* test was performed, when noted, by GraphPad Software. Differences of $P < 0.001$ were considered statistically different (24).

Results

Continuous exposure of PI-103 effectively suppresses the *in vitro* proliferation of EGFR mutant lung cancer cells in the presence of HGF

Both PC-9 and HCC827 cells were highly sensitive to continuous exposure (72 hours) to gefitinib and erlotinib. HGF alone did not affect proliferation of PC-9 cells, but it slightly stimulated the proliferation of HCC827 cells. Under these experimental conditions, HGF dose dependently induced resistance to gefitinib and erlotinib of PC-9 and HCC827 cells (Fig. 1), as reported previously (7). Under the same experimental conditions, continuous exposure (72 hours) of PI-103 inhibited the proliferation of PC-9 and HCC827 cells though the IC_{50} (half maximal inhibitory concentration) to PI-103 was higher (0.3 μmol/L for HCC827; 0.8 μmol/L for PC-9 cells) than gefitinib (0.01 μmol/L for HCC827; 0.03 μmol/L for PC-9 cells) and erlotinib (0.01 μmol/L for HCC827; 0.02 μmol/L for PC-9 cells). Importantly, HGF did not decrease the sensitivity of PC-9 and HCC827 cells to PI-103, suggesting the potential of PI-103 to overcome HGF-induced resistance to gefitinib and erlotinib *in vitro*.

We recently reported that HGF induces resistance in lung cancer cells (H1975) with *EGFR* T790M second mutation to irreversible EGFR-TKI that is expected to overcome T790M second-mutation–mediated resistance to gefitinib or erlotinib (25). Interestingly, continuous exposure (72 hours) of PI-103 inhibited proliferation of H1975 cells in a dose-dependent manner (Supplementary Fig. S1). HGF slightly stimulated proliferation of H1975 cells and induced the resistance to irreversible EGFR-TKI, CL-387,785 (N-[4-[(3-bromophenyl)amino]-6-quinazolinyl]-2-butynamide). However, HGF did not affect the sensitivity of H1975 cells to PI-103. These results suggest that PI-103 has potential to overcome HGF-induced resistance to not only reversible EGFR-TKIs but also irreversible EGFR TKIs. Moreover, combined use of PI-103 with CL-387,785 further inhibited proliferation of H1975 cells, irrespective of the presence of HGF.

We next examined whether PI-103 sensitized *EGFR* mutant lung cancer cells when combined with gefitinib in the presence or absence of HGF. PI-103 inhibited the proliferation of PC-9 and HCC827 cells in a dose-dependent manner. Gefitinib markedly suppressed the proliferation, and HGF induced the resistance to gefitinib. Surprisingly, PI-103 combined with gefitinib further inhibited the proliferation of PC-9 and HCC827 cells not only in the absence of HGF but also in the presence of HGF (Fig. 2A). Proliferation data were analyzed by the established method of Chou and Talalay (23) by using CalcuSyn software. The resulting CI values were les than 1 over most of the effect range of the drugs, demonstrating that the combination of PI-103 and gefitinib inhibited the proliferation synergistically in PC-9 and HCC827 cells. Same results were reproduced with GDC-0941–a derivative of PI103 with improved pharmacokinetic and pharmacodynamic properties that are active against all isoforms of class

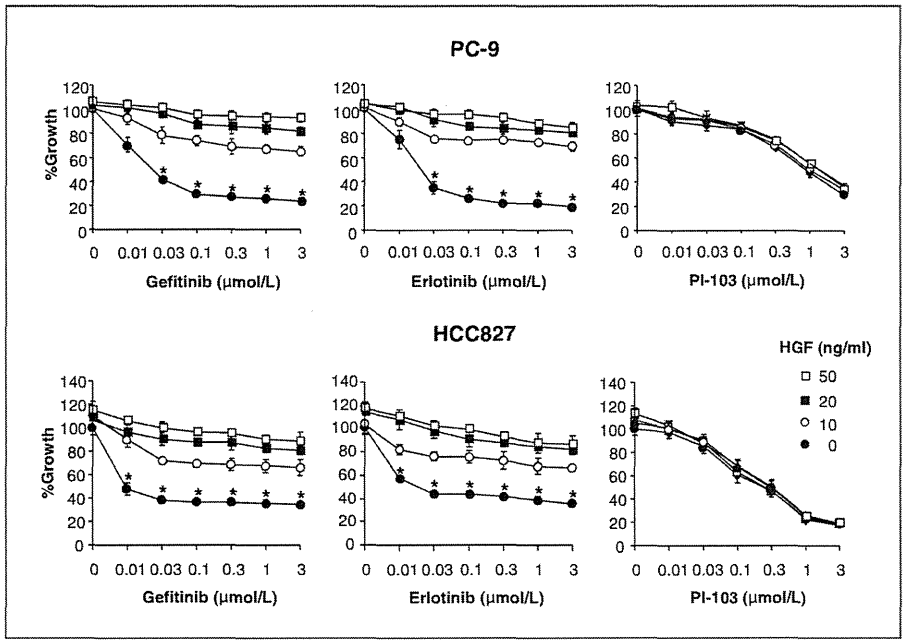

Figure 1. Continuous exposure of PI-103 suppresses the *in vitro* proliferation of *EGFR* mutant lung cancer cells, irrespective of the presence of HGF. Tumor cells were continuously treated with increasing concentrations of EGFR-TKI (gefitinib or erlotinib) or PI-103, with or without HGF, and cell growth was determined after 72 hours by MTT assay. Data shown are the representative of 5 independent experiments. Error bars indicate SD of triplicate cultures. *, $P < 0.001$ (Student's *t* test).

Published OnlineFirst January 10, 2011; DOI: 10.1158/1078-0432.CCR-10-1993

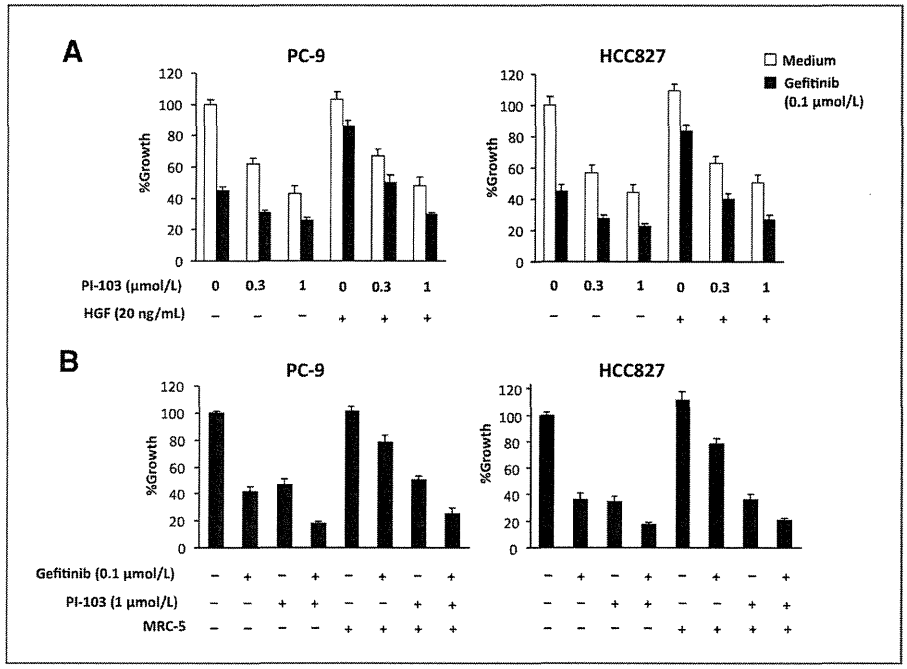

Figure 2. PI-103 combined with gefitinib overcomes HGF-induced gefitinib resistance *in vitro*. A, tumor cells were continuously treated with various concentrations of gefitinib and PI-103, with or without HGF, and cell growth was determined after 48 hours by MTT assay. B, tumor cells were cocultured with human lung fibroblasts (MRC-5) and were continuously treated with indicated concentrations of gefitinib, and/or PI-103. Cell growth was determined after 48 hours by MTT assay. Data shown are the representative of 3 independent experiments. Error bars indicate SD of triplicate cultures.

I PI3Ks and now used in clinical trials in patients with solid tumors (26; Supplementary Fig. 2). This synergy was also observed in a coculture system where HGF high producing fibroblasts, MRC-5, induced gefitinib resistance. While PI-103 did not inhibit HGF expression in MRC-5 cells (Supplementary Fig. S3), PI-103 synergistically inhibited the proliferation of PC-9 and HCC827 cells, irrespective of the presence of MRC-5 cells, when combined with gefitinib (Fig. 2B). These results suggest that PI3K inhibitor combined with gefitinib may be more beneficial than either monotherapy.

PI-103 with or without gefitinib suppresses PI3K/Akt pathway even in the presence of HGF

To explore the molecular mechanism by which PI-103 combined with gefitinib showed greater antiproliferative effect, we examined the phosphorylation of MET, EGFR, ErbB3, and their downstream pathways (PI3K/Akt and ERK1/2) by Western blotting (Fig. 3A). PC-9 and HCC827 cells expressed EGFR, ErbB3, and MET proteins, and these molecules were phosphorylated at various levels. These receptors and downstream molecules, such as Akt and ERK1/2, were also phosphorylated. While HGF alone did not affect phosphorylation of EGFR or ErbB3, it stimulated phosphorylation of MET and thereby activated Akt and ERK1/2. Although gefitinib inhibited phosphorylation of Akt and ERK1/2 in the absence of HGF, it failed to inhibited Akt and ERK1/2 phosphorylation in the presence of HGF. Importantly, PI-103 did not affect the phosphorylation of ERK1/2 or upstream molecules such as MET, EGFR, and ErbB3, but did inhibit the phosphotylation of Akt, regardless of presence of HGF. In addition, PI-103 combined with gefitinib inhibited phosphorylation of both Akt and ERK1/2 in the absence of HGF. The combination of PI-103 and gefitinib inhibited Akt phosphorylation, even in the presence of HGF, but failed to inhibit ERK1/2 phosphorylation. These results confirm our previous observations (7) and further suggest that PI-103 overcomes this resistance by inhibiting phosphorylation of downstream PI3K/Akt. The importance of PI3K/Akt as a target of PI-103 was further supported the evidence obtained in experiments with siRNA for Akt. Treatment with siAkt1 alone knocked down the Akt expression in PC-9 cells (Fig. 3B) and resulted in inhibition of cell proliferation by 20% (Fig. 3C). Notably, the treatment with siAkt1 reversed HGF-induced gefitinib resistance in combination with gefitinib (Fig. 3C).

PI-103 combined with gefitinib overcomes HGF-induced gefitinib resistance *in vivo*

We recently established an *in vivo* model by inoculating PC-9 cells premixed with HGF high producing MRC-5 cells and showed that gefitinib resistance that was abrogated by HGF-MET inhibition (9). By using this model, we next evaluated whether PI-103 overcomes HGF-induced resistance to gefitinib *in vivo*. Consistent with previous observations, we found that treatment with gefitinib alone prevented the enlargement of tumors produced by the mixture of PC-9 cells and MRC-5 cells, but did not cause tumor regression. Since gefitinib induces tumor shrinkage of PC-9 tumors (9), our results suggest that MRC-5 cells induced gefitinib resistance *in vivo*. Under these experimental conditions, treatment with PI-103 alone did not inhibit tumor growth, whereas combined treatment with PI-103 and gefitinib dramati-

Published OnlineFirst January 10, 2011; DOI: 10.1158/1078-0432.CCR-10-1993

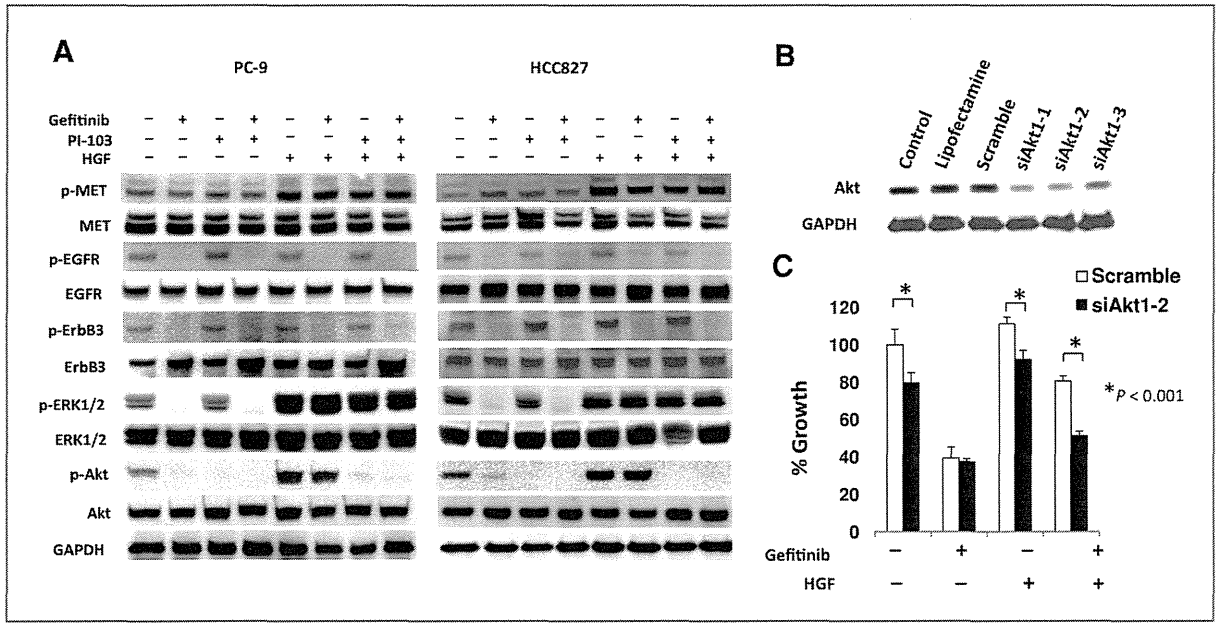

Figure 3. PI-103 with or without gefitinib suppresses PI3K/Akt pathway even in the presence of HGF. A, tumor cells were treated with or without gefitinib (1 μmol/L), PI-103 (1 μmol/L), and/or HGF (20 ng/mL) for 1 hour. Then, cells were lyzed, and the indicated proteins were detected by immunoblotting. Data shown are the representative of 3 independent experiments. B, PC-9 cells were treated with 3 different siRNAs specific for Akt1 or scramble siRNA. C, resultant cells were treated with gefitinib (0.1 μmol/L) and or HGF (20 ng/mL) for 48 hours. Then, MTT assay was performed. GAPDH, glyceraldehyde 3-phosphate dehydrogenase.

cally regressed the tumors (Fig. 4A and B). Similar results were reproduced by GDC-0941 that is now used in clinical trials in patients with solid tumors (Supplementary Fig. S4). These combined treatments did not cause obvious side effects, such as weight loss of the mice.

We further examined apoptotic cells in the tumors treated with gefitinib and/or PI-103. Although there were few apoptotic cells in control-treated (Fig. 4C) or PI-103–treated tumors (Fig. 4D), discernible numbers of apoptotic cells were detected in gefitinib-treated tumors (Fig. 4E). However, more apoptotic cells were found in tumors treated with both PI-103 and gefitinib (Fig. 4F; Fig. 4A and B). Immunoblots with these tumors revealed that treatment with PI-103 with or without gefitinib did not affect the phosphorylation of ERK1/2. On the other hand, PI-103 alone or in combination with gefitinib inhibited Akt phosphorylation in the tumor. Most notably, PI-103 combined with gefitinib induced cleaved caspase-3, the effector caspase that mediates death signaling (Fig. 4G). These results strongly suggested the importance of PI3K/Akt as a target of this combined therapy.

Short exposure of PI-103 combined with gefitinib further inhibits Akt mediating signal and proliferation of EGFR mutant lung cancer cells

Our finding that PI-103 monotherapy did not inhibit tumor growth, whereas PI-103 overcame synergistically HGF (MRC-5)-induced gefitinib resistance when combined with gefitinib, was unexpected. Although PI-103 has been reported to have very rapid tissue distribution and tissue clearance *in vivo* (half-life of PI-103 in the major organs is 0.7–1.3 hours; ref. 12), we hypothesized that rapid tissue clearance of PI-103 might be responsible for its insufficient therapeutic effect *in vivo*. To mimic pharmacodynamics of PI-103 *in vivo*, we exposed PC-9 and HCC827 cells to PI-103 transiently for 1 hour, washed the cells, and incubated the resultant cultures in fresh medium for 48 hours (Fig. 5A). Transient exposure to PI-103 resulted only in approximately 15% inhibition of the proliferation of PC-9 or HCC827 cells, whereas transient exposure to gefitinib resulted in higher inhibition of proliferation (>30%). Importantly, transient exposure to both PI-103 and gefitinib inhibited the proliferation of these 2 cell lines, reaching IC_{50} (Fig. 5B). Analysis using CalcuSyn software (23) indicates that the effect was synergistic. These phenomena were also observed when *EGFR* mutant cancer cells were cocultured with MRC-5 cells (Fig. 5C) to induce gefitinib resistance, representing the therapeutic efficacy seen *in vivo* model. In contrast, transient exposure to PI-103 and/or gefitinib did not inhibit proliferation of MRC-5 cells (Fig. 5D).

We further evaluated the kinetics of PI3K/Akt phosphorylation after transient exposure of PC-9 cells to PI-103 and gefitinib (Fig. 6A). As shown earlier (Fig. 3), 1 hour treatment with either PI-103 or gefitinib completely inhibited Akt phosphorylation in the absence of HGF. We found out that in the absence of HGF, gefitinib, alone or combined with PI-103, inhibited Akt phosphorylation for up to

Published OnlineFirst January 10, 2011; DOI: 10.1158/1078-0432.CCR-10-1993

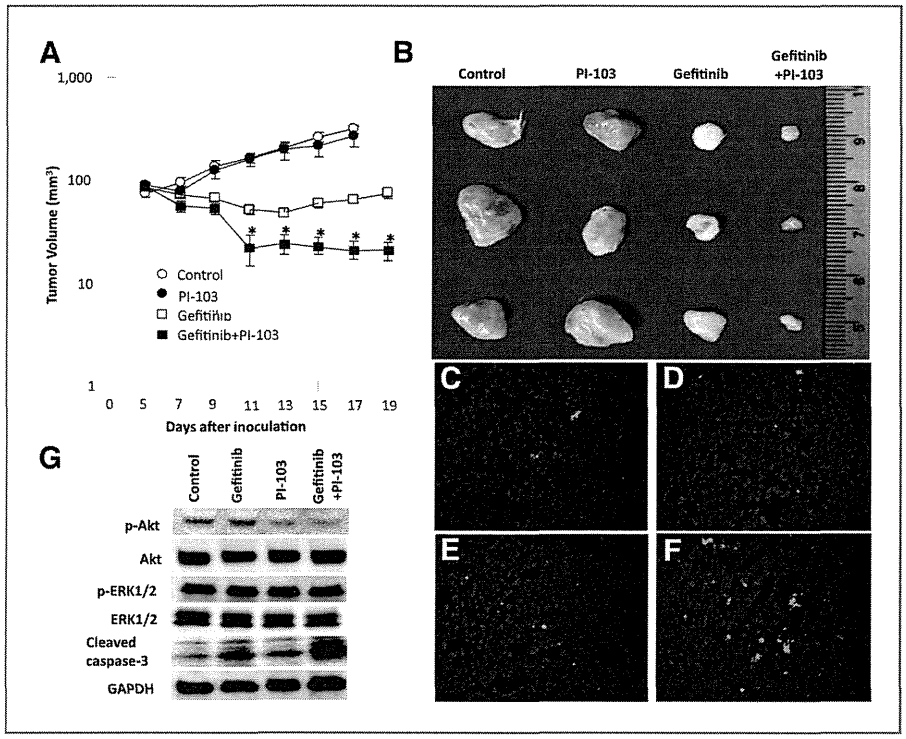

Figure 4. PI-103 combined with gefitinib overcomes HGF-induced gefitinib resistance *in vivo*. A, PC-9 cells (5×10^6) mixed with MRC-5 cells (5×10^6) were inoculated subcutaneously into SCID mice on day 0. Mice received oral gefitinib (25 mg/kg/d) and/or intraperitoneal PI-103 (5 mg/kg/d), starting on day 4. The tumor size was measured every 2 days and tumor volumes were calculated as described in Materials and Methods. Data shown are the representative of 2 independent experiments. Error bars indicate standard errors of 6 mice. *, $P < 0.001$ (Student's t test). B, macroscopic appearances of representative tumors harvested on day 19 are shown. Apoptotic cells were stained by TUNEL method as described in Materials and Methods. C, control. D, PI-103 alone. E, gefitinib alone. F, gefitinib + PI-103. G, tumors were harvested 1 hour after treatment on day 6. Tumor lysates were analyzed by immunoblotting with the indicated antibodies.

1 hour; subsequently, however, Akt phosphorylation in PC-9 cells treated with PI-103 alone started to recover. In the presence of HGF, gefitinib did not inhibit Akt phosphorylation, whereas Akt phosphorylation in PC-9 cells treated with PI-103 alone recovered by 1 hour after washing. However, cells treated with PI-103 plus gefitinib showed inhibition of Akt phosphorylation 1 hour after washing (Fig. 6A). More importantly, transient exposure to PI-103 plus gefitinib, but not either alone, resulted in the induction of cleaved caspase-9 and caspase-3, the initiator and effector caspases that mediate death signaling and cleaved PARP (Fig. 6A). Flow cytometry analyses with Annexin V further confirmed that transient exposure with PI-103 plus gefitinib induced apoptosis of HGF-treated PC-9 cells (Fig. 6B). These findings indicate that transient exposure to PI-103 combined with gefitinib is sufficient for inducing death signaling even in the presence of HGF, supporting the results observed *in vivo* experiments.

Discussion

Accumulating evidence indicate that HGF-MET axis is considerable therapeutic target for several solid tumors. HGF can act as autocrine growth factors for glioblastoma, thyroid cancer, and gastric cancer. Moreover, HGF stimulates the invasion and dissemination of various types of cancers (27), and inducing EGFR-TKI resistance in *EGFR* mutant lung cancer. In contrast to *MET* amplification–induced resistance, restoring the PI3K/Akt pathway and mediated by ErbB3 as an adaptor, HGF activates normal MET receptor and induces the resistance that restores PI3K/Akt pathway mediated by Gab1/2 as an adaptor (7–8). HGF also accelerates the expansion of preexisting clones with MET gene amplification and facilitates the induction of EGFR-TKI resistance in a population of *EGFR* mutant lung cancer (8). In addition, HGF frequently detected in EGFR-TKI–resistant tumors with *EGFR*-T790M second mutation and may induce the resistance to irreversible EGFR-TKIs (25). These observations highlight an important role of HGF ligand in controlling of tumor progression and drug sensitivity.

We have shown here that the combination of gefitinib and class I PI3K inhibitors, PI-103 and GDC-0941, overcame HGF-mediated gefitinib resistance in *EGFR* mutant lung cancer cells. Although HGF restored ERK1/2 and PI3K/Akt phosphorylation via MET activation even in the presence of gefitinib, transient exposure of PI-103 plus gefitinib efficiently inhibited PI3K/Akt phosphorylation, induced death signaling, and caused apoptosis of PC-9 cells. The combined treatment with PI-103 and gefitinib did not inhibit phosphorylation of ERK1/2 (Fig. 3) or STAT3 (data not shown). Recently, it was shown that transient potent inhibition of BCR-ABL kinase activity is associated with maximal clinical benefit in patients with chronic myelogenous leukemia (CML; ref. 28). Our results illustrate the possibility that transient double blockade of EGFR and PI3K may be useful for controlling HGF-induced resistance to EGFR-TKIs in *EGFR* mutant lung cancer.

A large number of PI3K inhibitors are developed and are being evaluated in the preclinical and clinical trials (18,

Published OnlineFirst January 10, 2011; DOI: 10.1158/1078-0432.CCR-10-1993

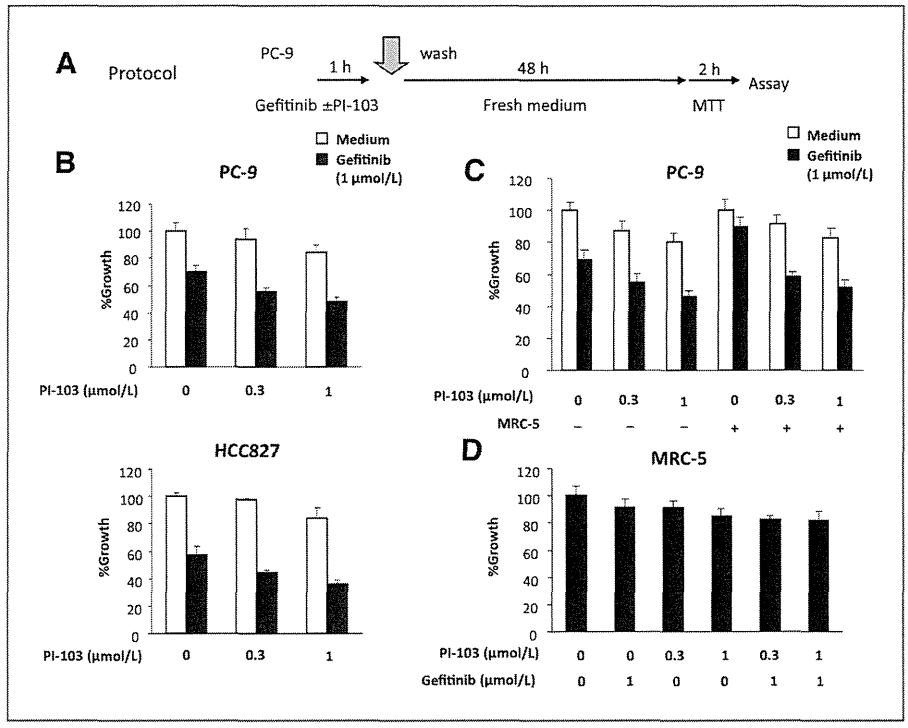

Figure 5. Short exposure of PI-103 combined with gefitinib effectively suppressed the proliferation of PC-9 and HCC827, but not MRC-5 cells. A, protocol. B, tumor cells were incubated with different concentrations of PI-103 and/or gefitinib for 1 hour, washed twice with PBS, and incubated in fresh medium for 48 hours. C, tumor cells were incubated with MRC-5 cells and different concentrations of PI-103 and/or gefitinib for 1 hour, washed twice with PBS, and coincubated with MRC-5 cells in fresh medium for 48 hours. D, MRC-5 cells were treated with different concentrations of PI-103 and/or gefitinib for 1 hour, washed twice with PBS, and further incubated in fresh medium for 48 hours. The cell growth was determined by MTT assay. Data shown are the representative of 3 independent experiments. Error bars indicate SD of triplicate cultures.

29). PI3K inhibitors have been found to induce G0/G1 cell arrest rather than apoptosis, and primarily causing stasis of tumor growth *in vivo* without substantial tumor shrinkage. For example, intraperitoneal administration of high doses of PI-103 (30–70 mg/kg) resulted in growth inhibition rather than regression in a range of human tumor xenografts (12, 30). Moreover, in *EGFR* mutant or *k-ras* mutant lung cancer models, tumor regression associating with apoptosis was observed only when PI3K/Akt pathway and MEK/MAPK pathway were simultaneously blocked (24, 31). Since these 2 pathways collaborate with each other to maintain cell survival, simultaneous blockade of both pathways is necessary to induce apoptosis. Surprisingly, our *in vitro* experiments revealed that though transient exposure of PI-103 plus gefitinib failed to inhibit ERK1/2 phosphorylation, it caused sustained PI3K/Akt inhibition, induced proapoptotic molecules, such as cleaved caspase-3 and caspase-9 and PARP, and thereby induced PC-9 cell apoptosis even in the presence of HGF. The mechanism by which combined use of PI-103 and gefitinib induces apoptosis of PC-9 cells, even in the presence of HGF, is not fully understood at present. One possible explanation is that double blockade of PI3K/Akt signaling pathway at upstream (EGFR level) and downstream (PI3K/Akt level) is efficient for inducing the apoptosis. The other possibility is that combined use of PI-103 and gefitinib inhibited the unknown pathway(s) that are responsible for survival of EGFR mutant lung cancer cells. While the combined therapy did not inhibit phosphorylation of STAT3 (data not shown) in PC-9 cells, we cannot rule out the involvement of other unknown pathway(s). Further experiments are warranted to clarify the mechanisms in future.

PI-103 is a class I PI3K inhibitor that reported favorable antitumor activity without any obvious side effects in preclinical animal models (12, 32). Pharmacokinetically, PI-103 is metabolized to form glucuronide and is cleared rapidly from plasma, with metabolysis of more than 70% PI-103 after 30 minutes of incubation with human and mouse microsomes (12). This is consistent with our results, showing that Akt phosphorylation in PC-9 cells treated with PI-103 alone was recovered by 1 hour (Fig. 6). PI-103 is not in clinical trials and work is now in progress to optimize its pharmacokinetics properties by structural modification (13). While continuous exposure for 72 hours of PI-103 inhibited the proliferation of PC-9 and HCC827 cells, transient exposure for 1 hour of PI-103 failed to do so *in vitro* condition. *In vivo* treatment with PI-103 (5 mg/kg intraperitoneally, once a day) also failed to inhibit the growth of PC-9 cells mixed with HGF high producing fibroblasts (MRC-5). Collectively, the insufficient effect of PI-103 monotherapy may be, at least in part, due to short half-life and rapid metabolism of this drug *in vivo*. GDC-0941 (5 mg/kg pharmacokinetics of oral, once a day) also failed to inhibit the growth of PC-9 cells mixed with MRC-5 cells. Though GDC-0941 is a derivative of PI103 with improved pharmacokinetic and pharmacodynamic properties, intratumoral concentration of GDC-0941 might not be enough to inhibit tumor growth in our *in vivo* experimental conditions. However, GDC-0941,

Published OnlineFirst January 10, 2011; DOI: 10.1158/1078-0432.CCR-10-1993

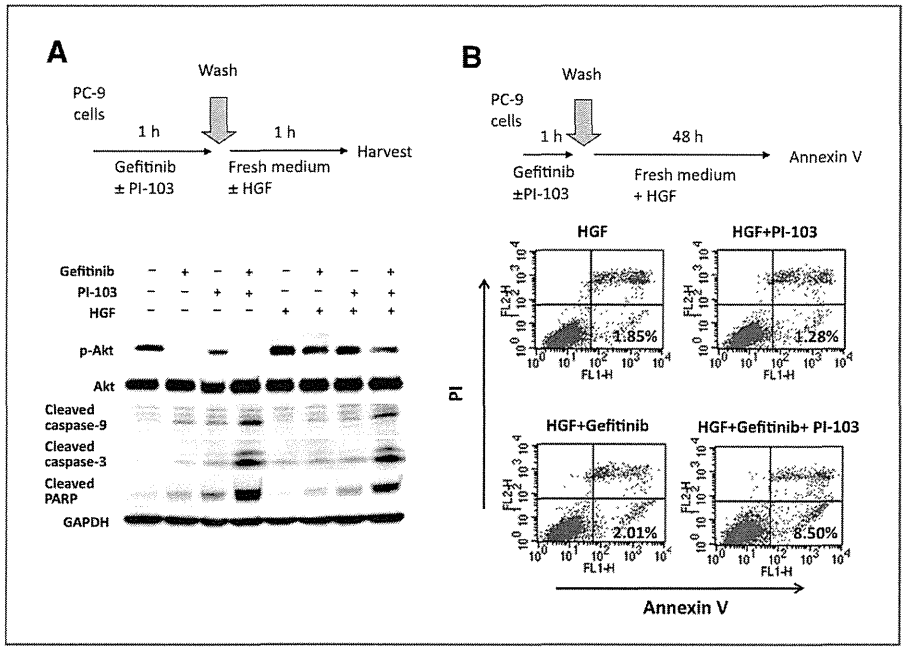

Figure 6. Apoptosis and time kinetics of phosphorylated Akt and proapoptotic molecules after short exposure to PI-103 and/or gefitinib. A, PC-9 cells were incubated (1 μmol/L), PI-103 (1 μmol/L), and/or HGF (20 ng/mL) for 1 hour. Then, the resultant cultures were incubated in fresh medium for 1 hour. Then, the cells were lyzed, and the indicated proteins were detected by immunoblotting. B, PC-9 cells were incubated with HGF (20 ng/mL) and PI-103 (1 μmol/L), and/or gefitinib (1 μmol/L), for 1 hour, and then washed 2 times with PBS. The resultant cultures were incubated in fresh medium for 24 hours. The apoptotic cells were determined by Annexin V assay kit according to manufactory protocol. Values shown are percentage of apoptotic cells. FL1-H and FL2-H, heights of fluorescence intensity.

like PI-103, successfully reversed the resistance when combined with gefitinib (Supplementary Fig. S4). Since we did not use maximum tolerated dose of these PI3K inhibitors (70–150 mg/kg; refs. 12, 26), our findings suggest that suboptimal dose of PI3K inhibitors may overcome HGF-induced resistance if combined with EGFR-TKIs.

In this study, we showed the possibility that double blockade of PI3K/Akt signaling pathway at upstream (EGFR level) and downstream (PI3K/Akt level) may be useful for overcoming HGF-induced resistance to EGFR-TKIs in *EGFR* mutant lung cancer cells. This concept can also be applicable to circumvent HGF-induced resistance to irreversible EGFR-TKIs (25). Moreover, cancer cell populations were recently shown to exhibit reversible tolerance to EGFR-TKIs by maintaining a phenotypical distinct subpopulation of cells that can protect the overall population from eradication by EGFR-TKIs (33). This reversible tolerance is mediated by activation of insulin like growth factor (IGF)-1 receptor (IGF-1R), but can be overcome by IGF-1R inhibitor combined with gefitinib ((35). Since PI3K/Akt is involved in IGF-1R–mediating signaling, the combined use of PI3K inhibitor may also protect against the emergence of reversibly tolerant subpopulations and may potently eradicate *EGFR* mutant lung cancer. Further investigations in PI3K/Akt signaling pathway are warranted for developing more successful compounds with better activity and safety for *EGFR* mutant lung cancer patients.

Disclosure of Potential Conflicts of Interest

No potential conflicts of interest were disclosed.

Acknowledgements

We thank Dr. J.D. Minna and Dr. Y. Sekido for kindly providing H1975 cells.

Grant Support

This study was supported by Grants-in-Aid of Cancer Research from the Ministry of Education, Science, Sports, and Culture of Japan (S. Yano, 21390256 and 22112010A01).

The costs of publication of this article were defrayed in part by the payment of page charges. This article must therefore be hereby marked *advertisement* in accordance with 18 U.S.C. Section 1734 solely to indicate this fact.

Received July 26, 2010; revised November 24, 2010; accepted December 18, 2010; published OnlineFirst January 10, 2011.

References

1. Pao W, Miller VA. Epidermal growth factor receptor mutations, small-molecule kinase inhibitors, and non-small-cell lung cancer: current knowledge and future directions. J Clin Oncol 2005;23:2556–68.
2. Mok TS, Wu YL, Thongprasert S, Yang CH, Chu DT, Saijo N, et al. Gefitinib or carboplatin-paclitaxel in pulmonary adenocarcinoma. N Engl J Med 2009;361:947–57.
3. Mitsudomi T, Morita S, Yatabe Y, Negoro S, Okamoto I, Tsurutani J, et al. Gefitinib versus cisplatin plus docetaxel in patients with non-small-cell lung cancer harbouring mutations of the epidermal growth factor receptor (WJTOG3405): an open label, randomised phase 3 trial. Lancet Oncol 2010;11:121–8.
4. Pao W, Miller VA, Politi KA, Riely GJ, Somwar R, Zakowski MF, et al. Acquired resistance of lung adenocarcinomas to gefitinib or erlotinib

Published OnlineFirst January 10, 2011; DOI: 10.1158/1078-0432.CCR-10-1993

is associated with a second mutation in the EGFR kinase domain. PLoS Med 2005;2:e73.
5. Kobayashi S, Boggon TJ, Dayaram T, Janne PA, Kocher O, Meyerson M, et al. EGFR mutation and resistance of non-small-cell lung cancer to gefitinib. N Engl J Med 2005;352:786–92.
6. Engelman JA, Zejnullahu K, Mitsudomi T, Song Y, Hyland C, Park JO, et al. MET amplification leads to gefitinib resistance in lung cancer by activating ERBB3 signaling. Science 2007;316:1039–43.
7. Yano S, Wang W, Li Q, Matsumoto K, Sakurama H, Nakamura T, et al. Hepatocyte growth factor induces gefitinib resistance of lung adenocarcinoma with epidermal growth factor receptor-activating mutations. Cancer Res 2008;68:9479–87.
8. Turke AB, Zejnullahu K, Wu YL, Song Y, Dias-Santagata D, Lifshits E, et al. Preexistence and clonal selection of MET amplification in EGFR mutant NSCLC. Cancer Cell 2010;17:77–88.
9. Wang W, Li Q, Yamada T, Matsumoto K, Matsumoto I, Oda M, et al. Crosstalk to stromal fibroblasts induces resistance of lung cancer to epidermal growth factor receptor tyrosine kinase inhibitors. Clin Cancer Res 2009;15:6630–8.
10. Onitsuka T, Uramoto H, Nose N, Takenoyama M, Hanagiri T, Sugio K, et al. Acquired resistance to gefitinib: the contribution of mechanisms other than the T790M, MET, and HGF status. Lung Cancer 2010;68: 198–203.
11. Matsumoto K, Nakamura T. Hepatocyte growth factor and the MET system as a mediator of tumor-stromal interactions. Int J Cancer 2006;119:477–83.
12. Raynaud FI, Eccles S, Clarke PA, Hayes A, Nutley B, Alix S, et al. Pharmacologic characterization of a potent inhibitor of class I phosphatidylinositide 3-kinases. Cancer Res 2007;67:5840–50.
13. Kong D, Yamori T. Phosphatidylinositol 3-kinase inhibitors: promising drug candidates for cancer therapy. Cancer Sci 2008;99:1734–40.
14. Engelman JA. Targeting PI3K signalling in cancer: opportunities, challenges and limitations. Nat Rev Cancer 2009;9:550–62.
15. Yamasaki F, Johansen MJ, Zhang D, Krishnamurthy S, Felix E, Bartholomeusz C, et al. Acquired resistance to erlotinib in A-431 epidermoid cancer cells requires down-regulation of MMAC1/PTEN and up-regulation of phosphorylated Akt. Cancer Res 2007;67:5779–88.
16. Ogino A, Kitao H, Hirano S, Uchida A, Ishiai M, Kozuki T, et al. Emergence of epidermal growth factor receptor T790M mutation during chronic exposure to gefitinib in a non small cell lung cancer cell line. Cancer Res 2007;67:7807–14.
17. Kharas MG, Janes MR, Scarfone VM, Lilly MB, Knight ZA, Shokat KM, et al. Ablation of PI3K blocks BCR-ABL leukemogenesis in mice, and a dual PI3K/mTOR inhibitor prevents expansion of human BCR-ABL+ leukemia cells. J Clin Invest 2008;118:3038–50.
18. Liu P, Cheng H, Roberts TM, Zhao JJ. Targeting the phosphoinositide 3-kinase pathway in cancer. Nat Rev Drug Discov 2009;8:627–44.
19. Inoue A, Suzuki T, Fukuhara T, Maemondo M, Kimura Y, Morikawa N, et al. Prospective phase II study of gefitinib for chemotherapy-naive patients with advanced non-small-cell lung cancer with epidermal growth factor receptor gene mutations. J Clin Oncol 2006;24:3340–6.
20. Yun CH, Mengwasser KE, Toms AV, Woo MS, Greulich H, Wong KK, et al. The T790M mutation in EGFR kinase causes drug resistance by increasing the affinity for ATP. Proc Natl Acad Sci U S A 2008;105: 2070–5.
21. Nakamura T, Nishizawa T, Hagiya M, Seki T, Shimonishi M, Sugimura A, et al. Molecular cloning and expression of human hepatocyte growth factor. Nature 1989;342:440–3.
22. Green LM, Reade JL, Ware CF. Rapid colorimetric assay for cell viability: application to the quantitation of cytotoxic and growth inhibitory lymphokines. J Immunol Methods 1984;70:257–68.
23. Chou TC, Talalay P. Quantitative analysis of dose-effect relationships: the combined effects of multiple drugs or enzyme inhibitors. Adv Enzyme Regul 1984;22:27–55.
24. Faber AC, Li D, Song Y, Liang MC, Yeap BY, Bronson RT, et al. Differential induction of apoptosis in HER2 and EGFR addicted cancers following PI3K inhibition. Proc Natl Acad Sci U S A 2009;106: 19503–8.
25. Yamada T, Matsumoto K, Wang W, Li Q, Nishioka Y, Sekido Y, et al. Hepatocyte growth factor reduces susceptibility to an irreversible epidermal growth factor receptor inhibitor in EGFR-T790M mutant lung cancer. Clin Cancer Res 2010;16:174–83.
26. Raynaud FI, Eccles SA, Patel S, Alix S, Box G, Chuckowree I, et al. Biological properties of potent inhibitors of class I phosphatidylinositide 3-kinases: from PI-103 through PI-540, PI-620 to the oral agent GDC-0941. Mol Cancer Ther 2009;8:1725–38.
27. Matsumoto K, Nakamura T. Mechanisms and significance of bifunctional NK4 in cancer treatment. Biochem Biophys Res Commun 2005;333:316–27.
28. Shah NP, Kasap C, Weier C, Balbas M, Nicoll JM, Bleickardt E, et al. Transient potent BCR-ABL inhibition is sufficient to commit chronic myeloid leukemia cells irreversibly to apoptosis. Cancer Cell 2008;14: 485–93.
29. Kong D, Yamori T. Advances in development of phosphatidylinositol 3-kinase inhibitors. Curr Med Chem 2009;16:2839–54.
30. Dan S, Yoshimi H, Okamura M, Mukai Y, Yamori T. Inhibition of PI3K by ZSTK474 suppressed tumor growth not via apoptosis but G0/G1 arrest. Biochem Biophys Res Commun 2009;379:104–9.
31. Engelman JA, Chen L, Tan XH, Crosby K, Guimaraes AR, Upadhyay R, et al. Effective use of PI3K and MEK inhibitors to treat mutant Kras G12D and PIK3CA H1047R murine lung cancers. Nat Med 2008;14:1351–6.
32. Fan QW, Knight ZA, Goldenberg DD, Yu W, Mostov KE, Stokoe D, et al. A dual PI3 kinase/mTOR inhibitor reveals emergent efficacy in glioma. Cancer Cell 2006;9:341–9.
33. Sharma SV, Lee DY, Li B, Quinlan MP, Takahashi F, Maheswaran S, et al. A chromatin-mediated reversible drug-tolerant state in cancer cell subpopulations. Cell 2010;141:69–80.

British Journal of Cancer (2011) 104, 505–513

www.bjcancer.com

Enhancement of osteoclastogenic activity in osteolytic prostate cancer cells by physical contact with osteoblasts

A Shiirevnyamba[1,2], T Takahashi[1], H Shan[1], H Ogawa[1], S Yano[3], H Kanayama[2], K Izumi[1] and H Uehara[*,1]

[1]Department of Molecular and Environmental Pathology, The University of Tokushima Graduate School, 3-18-15, Kuramoto-cho, Tokushima 770-8503, Japan; [2]Department of Urology, Institute of Health Biosciences, The University of Tokushima Graduate School, 3-18-15, Kuramoto-cho, Tokushima 770-8503, Japan; [3]Division of Medical Oncology, Cancer Research Institute, Kanazawa University, Kanazawa, Ishikawa 920-0934, Japan

BACKGROUND: The interaction between prostate cancer cells and osteoblasts is critical for the development of bone metastasis. Metastatic cancer cells may physically contact osteoblasts in the bone microenvironment; however, the biological significance of this interaction is not fully understood.

METHODS: Human prostate cancer cells (the osteolytic cell line PC-3 and the osteoblastic cell line MDA-PCa 2b) and human osteoblasts (hFOB1.19) were cocultured under two different conditions (bilayer and contact conditions). Differential gene expression profiles of prostate cancer cells were then investigated using microarray analysis. Differentially expressed genes were analysed using RT–PCR and western blotting, and the effect of anti-cadherin neutralising antibodies on their expression was assayed. The osteoclastogenic activity of cells grown under these different conditions was also investigated using an *in vitro* assay.

RESULTS: When PC-3 or MDA-PCa 2b cells were cocultured with hFOB1.19 cells under contact conditions, the expression of eight genes was upregulated and that of one gene was downregulated in PC-3 cells compared with gene expression in bilayer culture. No differentially expressed genes were detected in MDA-PCa 2b cells. Four of the eight upregulated genes (interleukin-1β (IL-1β), cyclooxygenase-2 (COX-2), IL-6 and the third component of complement (C3)) have already been reported to participate in osteoclastogenesis. Indeed, a cell lysate of PC-3 cells grown under contact coculture conditions significantly enhanced osteoclastogenesis *in vitro* ($P<0.005$). neutralisation of cadherin-11 with a specific antibody inhibited upregulation of COX-2 and C3 mRNA in PC-3 cells. In contrast, neutralisation of N-cadherin induced upregulation of COX-2 mRNA.

CONCLUSION: Physical contact between osteolytic prostate cancer cells and osteoblasts may upregulate osteoclastogenesis-related gene expression in prostate cancer cells and enhance osteoclastogenesis. Additionally, cadherin-11 and N-cadherin are involved in this process. These data provide evidence supporting new therapies of prostate cancer bone metastasis that target direct cancer-cell-osteoblast cell–cell contact.

British Journal of Cancer (2011) **104,** 505–513. doi:10.1038/sj.bjc.6606070 www.bjcancer.com
Published online 4 January 2011

Keywords: physical contact; cell-to-cell interaction; prostate cancer; bone metastasis; osteoclastogenesis

Prostate cancer continues to be the most common cancer, and the second leading cause of cancer deaths, among American men. Despite earlier diagnosis and refinements in surgery and radiation, it was estimated that 28 660 men would die from prostate cancer in the United States in 2008 (Jemal *et al*, 2008). Moreover, there has been a recent trend towards an increased incidence of prostate cancer in Asia, although the rate of prostate cancer in Asia is still much lower than that in the United States or in many European countries (Sim and Cheng, 2005). Bone metastasis of prostate cancer is the major cause of morbidity and mortality, and was detected at autopsy in up to 90% of patients who died from prostate cancer (Bubendorf *et al*, 2000). Metastasis of prostate cancer cells to bone is a multistep process including detachment of cancer cells from the primary site, travel of the cells in the blood or lymph, attachment to bone tissue and development of a tumour at the site of the bone metastasis. Prostate cancer metastases cause an osteoblastic (excessive bone forming), osteolytic (bone lysing) or mixed bone response (Charhon *et al*, 1983; Cheville *et al*, 2002; Roudier *et al*, 2003).

The interaction between prostate cancer cells and normal cells in a bone microenvironment is important for survival and proliferation of metastatic cancer cells. It has been shown that factors secreted by prostate cancer cells alter bone homoeostasis by disrupting a balance between osteoblastic and osteoclastic activity (Roudier *et al*, 2003; Logothetis and Lin, 2005; Morrissey *et al*, 2010). In turn, osteoblasts and osteoclasts secrete factors that facilitate progression of prostate cancer in bone (Lang *et al*, 1995; Yin *et al*, 2005). Once prostate cancer cells have metastasised to bone marrow, the cancer cells are suspected to interact with osteoblasts, osteoclasts and stromal cells thorough both soluble factors and physical contact. Interaction mediated by soluble factors has been studied using *in vitro* coculture systems. In those studies, the conditioned medium of cancer cells, or bilayer condition using a cell culture insert, was used for coculture

*Correspondence: Dr H Uehara;
E-mail: uehara@basic.med.tokushima-u.ac.jp
Received 16 July 2010; revised 15 October 2010; accepted 1 December 2010; published online 4 January 2011

(Martínez *et al*, 1996; Kido *et al*, 1997; Hullinger *et al*, 2000; Fizazi *et al*, 2003). However, there have been few studies of the mechanism by which prostate cancer cells physically contact normal cells in a bone microenvironment. Wang *et al* (2006) established a novel physical contact coculture system and showed that physical contact between prostate cancer cells and bone marrow stromal cells may act as an independent factor affecting the progression of bone metastasis. However, interaction between prostate cancer cells and other normal cells in the bone microenvironment remains unclear.

A variety of factors, such as morphogenetic proteins, adhesion molecules, chemotactic factors, cytokines and growth factors, are known to be involved in the metastasis of prostate cancer to bone (Mundy, 2002; Roodman, 2004). Adhesion molecules, in particular, may have a crucial role in the interaction between prostate cancer cells and normal cells in the bone microenvironment. N-cadherin and cadherin-11 are highly expressed in prostate cancer cells and osteoblasts, but not in normal prostate tissue. Cadherin-11 promotes bone metastasis in a mouse model and its expression increases as the tumour progresses from primary prostate cancer to metastatic disease in lymph nodes and especially in bone (Gravdal *et al*, 2007; Chu *et al*, 2008). Therefore, heterotypic interactions between cancer cells and osteoblasts mediated through homophilic adhesion molecules may have a role in bone metastasis formation and progression, although the underlying mechanisms are not fully understood. It is absolutely crucial to precisely understand these molecular mechanisms in order to develop new therapies for bone metastasis.

In this study, we compared gene expression of prostate cancer cells that produce either osteoblastic or osteolytic lesions, after coculture with osteoblasts using two different coculture systems. Our study reveals that physical contact between osteolytic prostate cancer cells and osteoblasts may upregulate the expression of specific osteoclastogenesis-related genes in prostate cancer cells and enhance osteoclastogenesis. Additionally, at least in part, this process is cadherin-11 dependent.

MATERIALS AND METHODS

Histological analysis of bone metastasis in autopsy cases

A total of 229 autopsy cases were reviewed and 37 various cancer cases with bone metastasis (including two of prostate cancer) were selected for further analysis. Autopsies had been performed at Tokushima University Hospital between 2003 and 2008.

Cells and animals

The PC-3 human prostate cancer cell line was obtained from the Health Science Research Resources Bank (Osaka, Japan). The MDA-PCa 2b human prostate cancer cell line and hFOB1.19 immortalised human osteoblastic cell line were from the American Type Cell Culture Collection (Manassas, VA, USA). Both the PC-3 and the MDA-PCa 2b cell line were established from bone metastases, but the *in vivo* growth pattern of PC-3 cells is osteolytic (Uehara *et al*, 2003), whereas that of MDA-PCa 2b cells is osteoblastic (Fizazi *et al*, 2003). The hFOB1.19 cells were transfected with a gene coding for a temperature-sensitive mutant (tsA58) of the SV40 large T antigen and exhibit rapid growth at 33.5°C (Harris *et al*, 1995). Before coculture studies, we confirmed the mRNA expression of alkaline phosphatase and osteocalcin, markers of osteoblastic differentiation, in hFOB1.19 cells at 37°C using RT–PCR (data not shown). The PC-3 cell line was maintained in MEM supplemented with 10% fetal bovine serum (FBS), MDA-PCa 2b was maintained in BRFF-HPC1 (Athena Environmental Sciences, Baltimore, MD, USA) with 20% FBS and hFOB1.19 was maintained in phenol red-free DMEM/F12 supplemented with 10% FBS. Penicillin G (100 U ml^{-1}) and streptomycin sulphate (0.1 mg ml^{-1}) were added to all conditioned media. Male BALB/c mice (6–10 weeks old) and BALB/c nude mice (5 weeks old) were purchased from Crea Japan (Tokyo, Japan). Mice were housed and maintained under specific pathogen-free conditions. Experiments were performed according to the Guideline for the Care and Use of Laboratory Animals of the University of Tokushima School of Medicine, and were approved by the Animal Care and Use Committee.

Xenograft model of osteolytic bone metastasis

PC-3 cells (5×10^5 per mice) were injected into the proximal tibiae of nude mice under anaesthesia that consisted of a mixture of ketamine hydrochloride and xylazine. After 5–9 weeks, the mice were killed and the hind limbs were excised at the knee joint, fixed in 10% phosphate-buffered formaldehyde at room temperature for 24 h, and then decalcified with 10% EDTA (pH 7.4) at 4°C for 2 weeks. The tissues were then embedded in paraffin, sectioned and subjected to H&E staining and immunohistochemical staining.

Coculture assay and fluorescence-activated cell sorting

Prostate cancer cells and hFOB1.19 cells were cocultured in contact and bilayer cocultures. Before coculture, the prostate cancer cells (PC-3 and MDA-PCa 2b cells) and hFOB1.19 cells were treated with 10 μg ml^{-1} of the fluorescent dye $DiOC_{18}(3)$ or $DiIC_{18}(3)$ (Invitrogen, Carlsbad, CA, USA) for 48 h. In the contact coculture, the prostate cancer cells were mixed and cocultured with hFOB1.19 cells in serum- and phenol red-free DMEM/F12 for 48 h. The initial ratio of the cell numbers was set at 1 : 1. In the bilayer coculture, the prostate cancer cells were first seeded onto a 6-well plate (4×10^5 cells per well) and a cell culture insert (PET membrane, 0.4 μm pore size, Falcon, Franklin Lakes, NJ, USA) was subsequently placed on the top of each well. Equal numbers of hFOB1.19 cells were seeded onto this insert and the plate was cultured for 48 h. The medium used for this bilayer coculture was the same as that used for the contact coculture. In both types of coculture, the cells were harvested using 1 mM EDTA. Prostate cancer cells were isolated from the cocultured cell mixture using fluorescence-activated cell sorting (FACS) and the EPICS XL-MCL (Beckman Coulter, Fullerton, CA, USA). The osteoblast fraction was simultaneously isolated.

Immunocytochemical staining

After contact coculture, some of the isolated prostate cancer cells and osteoblasts were reseeded onto MAS-coated slide glass (Matsunami Glass Ind., Osaka, Japan) and were incubated at 37°C for 24 h. These cells were fixed in 95% ethanol at room temperature for 20 min, and were then heated in 0.01 M citrate buffer (pH 6.0) for 10 min in a pressure cooker for antigen retrieval. Immunocytochemical staining was performed using the ChemMate ENVISION kit/horseradish peroxidase (DakoCytomation, Carpenteria, CA, USA). A monoclonal SV40 T antigen antibody (PAb416; Calbiochem, Darmstadt, Germany), that reacts specifically with the SV40 large T antigen but not with SV40 small T antigen, was added to the slides at a dilution of 1 : 100, and was incubated for 1 h at room temperature. After washing with PBS, each slide was treated with horseradish peroxidase-conjugated secondary antibody for 40 min. The signal was visualized using 3, 3′-diaminobenzidine, and the cells were then counterstained with hematoxylin.

Microarray analysis

Total RNA from hFOB1.19, PC-3 and MDA-PCa 2b cells was isolated using an RNeasy Mini kit (QIAGEN, Valencia, CA, USA).

Table 1 Primers for RT–PCR

Marker	Forward (5′–3′)	Reverse (5′–3′)	Size (bp)	Reference
COX-2	CGCAGTACAGAAAGTATC	CTCTGGATCTGGAACAC	433	Takahashi *et al*, 2008
IL-1β	GAGCTCGCCAGTGAAATG	TGCATCGTGCACATAAGC	336	Takahashi *et al*, 2008
IL-6	AATTCGGTACATCCTCGAC	TTCTGTGCCTGCAGCTTC	381	Takahashi *et al*, 2008
C3	CAGGCAGCATCACTAAAG	CCTTGGTCTCTTCTGATC	480	Original
N-cadherin	GACAACATTCACTGCTCA	GAACTTCATAGATACCAG	488	Original
Cadherin-11	CAAGTTACATCCACGAAG	ATCTCGGTTGTCTCTGAC	488	Original
β-actin	TACAATGAGCTGCGTGTGG	AGATGGGCACAGTGTGGG	226	Takahashi *et al*, 2008

Relative purity of the RNA was measured using an Agilent 2100 Bioanalyzer (Agilent Technologies, Santa Clara, CA, USA). RNA expression was analysed using a GeneChip Human Gene 1.0 ST Array (Affymetrix, Santa Clara, CA, USA). This microarray chip contains 28 869 oligonucleotide probes for known and unknown genes. First strand cDNA was synthesised from 300 ng of total RNA using GeneChip whole transcript (WT) cDNA Synthesis and Amplification kit (Affymetrix) according to the manufacturer's protocol. Complementary RNA (10 μg) was input into the second-cycle cDNA reaction and then this cDNA was fragmented and end-labeled with the GeneChip WT Terminal Labelling kit (Affymetrix). Approximately 5.5 μg of labelled DNA target was hybridised to the Affymetrix GeneChip Human Gene 1.0 ST Array at 45°C for 17 h on a GeneChip Hybridisation 640 (Affymetrix) according to the manufacturer's recommendation. Hybridized arrays were washed and stained on a GeneChip Fluidics Station 450, were scanned using a GeneChip Scanner 3000 7G (Affymetrix) and then CEL files were generated for each array. This analysis was supported by the Support Center for Advanced Medical Sciences, the University of Tokushima Graduate School, Institute of Health Biosciences.

Semiquantitative RT-PCR

RNA molecules identified in the microarray analysis were subjected to semiquantitative RT-PCR analysis. Aliquots (2 μg per reaction) were reverse-transcribed using SuperScript II reverse transcriptase and random hexamers (Invitrogen). This reaction was conducted at 42°C for 60 min, after which the temperature was increased to 72°C for 15 min. The total cDNA was then amplified using PCR by following a thermocycling program of 94°C for 10 min for initial denaturation, 28 cycles of 94°C for 30 s, 55°C for 1 min, 72°C for 1 min for amplification, and a final extension at 72°C for 10 min. The sequences of these primers are listed in Table 1. The RT-PCR products were separated by 1.5% agarose gel electrophoresis and were visualized using an UV transilluminator.

ELISA and western blot analysis

After sorting, cocultured PC-3 cells were resuspended in phosphate-buffered saline containing 1 mM phenylmethylsulfonyl fluoride and were lysed using an ultrasonic homogenizer. These homogenates were then centrifuged and the supernatants were used as protein samples. The protein concentrations of the samples were quantified using the DC Protein Assay kit (Bio-Rad, Hercules, CA, USA). Aliquots (8 μg protein) were subjected to ELISA assays for IL-1β (Human IL-1β ELISA kit, Invitrogen), IL-6 (Quantikine human IL-6 immunoassay kit, R&D Systems, Minneapolis, MN, USA) and C3 (AssayMax human complement C3 ELISA kit, Assaypro, St Charles, MO, USA). Aliquots (10 μg protein) were also subjected to western blot analysis as described previously (Takahashi *et al*, 2008). Rabbit anti-COX-2 (Santa Cruz Biotechnology, Santa Cruz, CA, USA) and anti-actin (Sigma, St Louis, MO, USA) antibodies were used as the primary antibodies. Goat anti-rabbit IgG-horseradish peroxidase (Invitrogen) was employed as the secondary antibody. The dilutions used are as follows: anti-COX-2, 1:250; anti-actin, 1:10 000; and anti-rabbit IgG-horseradish peroxidase, 1:200 000. An immobilon western horseradish peroxidase substrate (Millipore, Billerica, MA, USA) was used to detect the signals.

Immunohistochemical staining

Paraffin sections (4 μm) of bone lesions from a xenograft model of osteolytic bone metastasis were deparaffinized in xylene and dehydrated through descending concentrations of ethanol. Antigen retrieval and immunostaining was performed according to the immunocytochemical staining protocol described above. A monoclonal mouse anti-COX-2 antibody (COX 229; Invitrogen) was used as the primary antibody at dilution of 1:50.

In vitro osteoclastogenesis assay

Bone marrow was collected from male BALB/c mice by flushing the femurs and tibias with serum-free DMEM. The cells were then washed twice in the same medium, were seeded onto a 100 mm dish and were cultured in 10% FBS-containing DMEM at 37°C for 1 week. During culture, the medium was changed every three days. Adherent cells were reseeded onto a 96-well microplate (1×10^4 cells per well), were preincubated at 37°C for 24 h and were then treated with each cell lysate from PC-3 cells cocultured with hFOB 1.19 cells under contact or bilayer conditions (10 μg) in the presence of receptor activator for nuclear factor-κB ligand (RANKL, R & D systems, Mineapolis, MN, USA) and macrophage colony-stimulating factor (M-CSF) (10 ng ml^{-1}; R&D Systems) after changing to flesh complete medium. After incubation for 10 days, the cells were fixed in 5% phosphate-buffered formaldehyde at room temperature for 5 min and tartrate-resistant acid phosphatase (TRAP) staining was conducted to detect differentiated osteoclasts. The composition of the TRAP staining solution was described in our previous report (Takahashi *et al*, 2008). The number of TRAP-positive cells in more then five microscopic fields was counted at × 200 magnification.

Neutralisation assay

PC-3 and hFOB1.19 cells were treated with $DiOC_{18}(3)$ and $DiIC_{18}(3)$, respectively. The conditions of treatment were the same as described above. Before contact coculture, the hFOB1.19 cells were treated with 40 μg ml^{-1} of neutralising anti-N-cadherin (Sigma) or anti-Cadherin-11 (R&D Systems) antibody, or of the corresponding isotype IgG for 30 min at 37°C. These antibody-treated hFOB1.19 cells and PC-3 cells were mixed and cocultured in serum- and phenol red-free DMEM/F12 for 48 h. The initial ratio of cell numbers was set at 1:1. PC-3 cells were isolated using FACS sorting as described above. Isolated PC-3 cells were used for semiquantitative RT-PCR analyses for COX-2, IL-1β, IL-6 and C3 mRNA. Calculations of signal intensities were performed by using NIHimage 1.62 software (http://rsbweb.nih.gov/nih-image/).

Statistical analyses

A two-tailed Student's *t*-test was employed for statistical analyses of the data. Significant results were determined at a $P<0.05$.

RESULTS

Histological findings of direct cancer-cell-osteoblast contact in bone metastasis

We first determined if cancer-cell-osteoblast cell–cell contact could be observed in bone lesions in a xenograft model of osteolytic bone metastasis. Bone surfaces facing tumours were extensively lysed by osteoclasts. However, in some areas, residual osteoblasts were observed very close to cancer cells suggesting direct cancer-cell-osteoblast contact (Figure 1A and B).

We next determined how often direct cancer-cell-osteoblast contact occurs in human tumours, by reviewing H&E-stained slides of 37 autopsy cases with bone metastases. The primary tumour sites of these cases were as follows: lung (17 cases), large intestine (4 cases), gallbladder (3 cases), pancreas, bladder and prostate (2 cases each), pleura, breast, stomach, liver, bile duct, kidney and soft tissue (1 case each). The bone metastases in the two case of prostate cancer were osteoblastic, and those in the other cases were osteolytic. The close proximity of cancer cells to osteoblasts suggesting direct cancer-cell-osteoblast contact was also observed to varying extents in all cases (Figure 1C and D).

Immunocytochemical staining of the SV 40 large T antigen

To further analyze cancer-cell-osteoblast contact, the human prostate cancer cells (PC-3 and MDA-PCa 2b calls) and hFOB1.19 osteoblasts, which were labelled with 10 $\mu g\,ml^{-1}$ of the fluorescent dye $DiOC_{18}(3)$ and $DiIC_{18}(3)$, respectively, were cocultured in contact or in bilayer cocultures for 48 h. Following coculture in contact cocultures, the prostate cancer cells and osteoblasts were then separated by sorting for further analyses. To confirm the purity of separated cell populations ($DiOC_{18}(3)$-labeled human prostate cancer cells and $DiIC_{18}(3)$-labeled human osteoblasts) after sorting, the cells were immunocytochemically stained for the SV40 large T antigen, which is a marker of hFOB1.19 cells. As shown in Figure 2, the nuclei of hFOB1.19 cells ($DiOC_{18}(3)^-$/$DiIC_{18}(3)^+$) stained positive for the SV40 large T antigen, whereas no positive staining of PC-3 or MDA-PCa 2b cells ($DiOC_{18}(3)^+$/$DiIC_{18}(3)^-$) was observed (MDA-PCa 2b cells are not shown in Figure 2). Thus, prostate cancer cells and osteoblasts can be completely separated by sorting after coculture in contact cocultures.

Gene expression analysis

We next performed cDNA microarray analysis of prostate cancer cells that had been cocultured with osteoblasts, to identify differential gene expression in prostate cancer cells because of physical contact with the osteoblasts. We compared gene expression in cocultures of both osteoblastic (MDA-PCa 2b) and osteolytic (PC-3) prostate cancer cell lines with osteoblasts under bilayer and contact culture conditions. As controls, the prostate cancer cells were cultured alone in the absence of osteoblasts. Under bilayer coculture conditions, there is no physical contact between the prostate cancer cells and the osteoblasts, but each cell line is exposed to soluble factors secreted by both cell types. In contrast, under contact coculture conditions, cancer cells and osteoblasts are both physically in contact and are exposed to soluble factors secreted by both cell types. The control prostate cancer cells cultured alone have no interaction with osteoblasts. The microarray results of the prostate cancer cells cultured alone were compared with those of prostate cancer cells from the bilayer

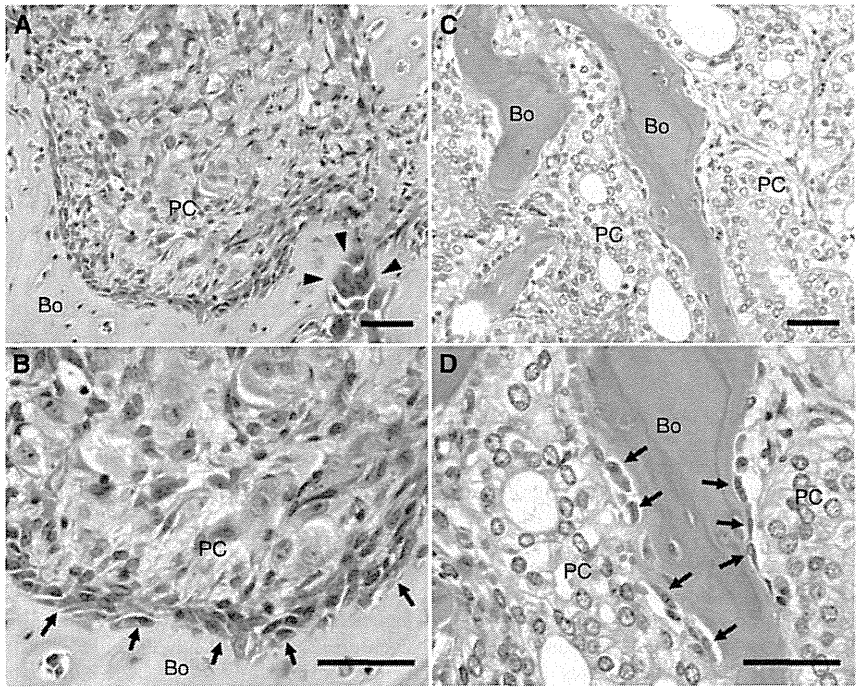

Figure 1 Histological findings suggesting direct prostate cancer-cell-osteoblast contact in bone metastases. The indicated tissues were fixed and analysed following H&E staining. (**A** and **B**) An osteolytic lesion produced by the growth of PC-3 human prostate cancer cells in the tibia of a nude mouse. The close proximity of PC-3 cells to osteoblasts suggesting direct cancer-cell-osteoblast contact, as well as osteolysis by osteoclasts was observed. (**C** and **D**) Representative osteoblastic bone metastases of autopsy cases of prostate cancer. The close proximity of prostate cancer cells to osteoblasts suggesting direct cancer-cell-osteoblast contact was also observed. Arrows, osteoblasts; arrow heads, osteoclasts; Bo, bone; PC, prostate cancer cells. Scale = 50 μm.

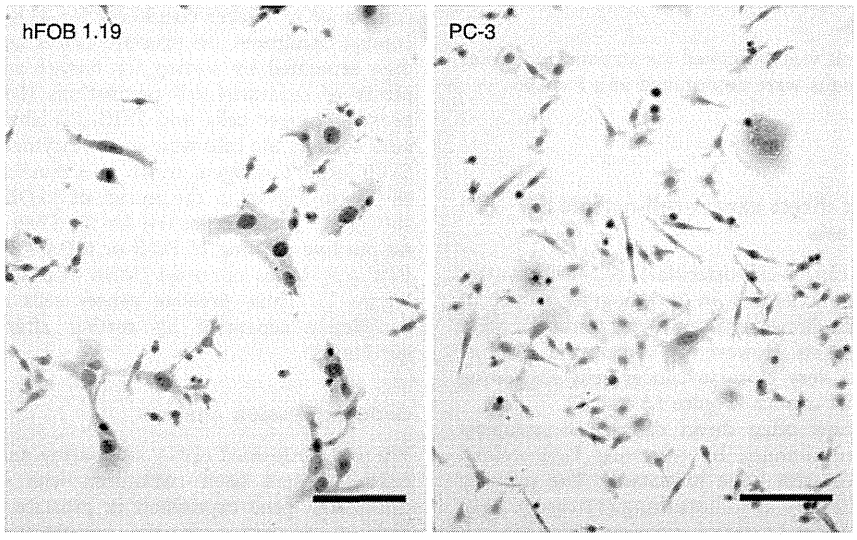

Figure 2 Immunohistochemical analysis of the SV40 large T antigen after sorting of cells in contact cocultures. PC-3 human prostate cancer cells (labelled with $DiOC_{18}(3)$) were mixed and cocultured with $DiIC_{18}(3)$-labeled human osteoblasts expressing SV40 (hFOB1.19) for 48 h. Cocultured prostate cancer cells ($DiOC_{18}(3)^{+}/DiIC_{18}(3)^{-}$) and hFOB1.19 cells ($DiOC_{18}(3)^{-}/DiIC_{18}(3)^{+}$) were then separated using flow cytometry. One thousand cells from each sorted cell population were cultured overnight on glass slides and were then immunohistochemically stained for the SV40 large T antigen. Positive staining of the SV40 large T antigen was observed in the nuclei of hFOB1.19 cells ($DiOC_{18}(3)^{-}/DiIC_{18}(3)^{+}$) but not in PC-3 cells ($DiOC_{18}(3)^{+}/DiIC_{18}(3)^{-}$). Scale = 100 μm.

Table 2 Up-/downregulated genes in PC-3 cells cultured under contact coculture conditions, identified by cDNA microarray analysis

Gene bank accession no.	Gene name	Fold change[a]
Upregulated genes in contact coculture conditions		
NM_007115	Tumor necrosis factor, alpha-induced protein 6	5.3
NM_000576	Interleukin 1-β	4.4
NM_000963	Prostaglandin-endoperoxide synthase 2 (COX2)	4.2
NM_001442	Fatty acid binding protein 4, adipocyte	4.0
NM_000600	Interleukin 6 (interferon, β-2)	3.7
NM_007028	Tripartite motif-containing 31	3.5
NR_003006	Small Cajal body-specific RNA 6 on chromosome 2	3.4
NM_000064	Complement component 3	3.2
Downregulated genes in contact coculture conditions		
NM_003118	Secreted protein, acidic, cysteine-rich (osteonectin)	0.3

[a]The microarray results of PC-3 cells in the contact coculture were compared with those of cells from the bilayer coculture. The fold change in gene expression that was >3.0 or <0.33 was considered significant.

coculture. The results of the prostate cancer cells in the bilayer coculture were further compared with those of cells from the contact coculture. A fold change in gene expression that was >3.0 or <0.33 was considered significant. There was no significant difference in gene expression between PC-3 cells cultured alone and those cocultured under bilayer conditions. This result suggested that soluble factors presents in the coculture did not affect the gene expression in PC-3 cells. In contrast, when the gene expression of PC-3 cells cultured under contact coculture conditions was compared with that of PC-3 cells cultured under bilayer coculture conditions, eight upregulated genes (3.2–5.3-fold) and one downregulated gene (0.3-fold) were identified in the contact cocultures (Table 2). Thus, the expression of these genes appeared to be specifically regulated by direct contact between PC-3 cells and osteoblasts. We then determined if these regulated genes might be related to genes that are known to be involved in cancer metastasis and bone remodelling. Four of the eight upregulated genes (IL-1β, COX-2, IL-6 and C3) have already been reported to participate in osteoclastogenesis (Mangham *et al*, 1993; Sato *et al*, 1993; García-Moreno *et al*, 2002; Roodman, 2004; Liu *et al*, 2005; Singh *et al*, 2007; Bussard *et al*, 2008). There was no significant difference in the gene expression of MDA-PCa 2b cells under any culture conditions.

Validation of cDNA microarray results

To confirm the microarray results, the mRNA expression of the four osteoclastogenesis-related genes that were upregulated in PC-3 cells following coculture with hFOB1. A total of 19 cells under contact conditions were examined using RT–PCR. Consistent with the cDNA microarray results, upregulation of IL-1β, COX-2, IL-6 and C3 mRNA were detected in PC-3 cells under contact coculture conditions compared with under bilayer coculture conditions (Figure 3A).

We next determined the expression of IL-1β, COX-2, IL-6 and C3 in PC-3 cells at the protein level. The protein levels of IL-1β, IL-6 and C3 were measured using ELISA. A PC-3 cell lysate was used for ELISA, rather than culture supernatant, to eliminate the influence of exogenous IL-1β, IL-6 and C3 secreted by osteoblasts in the coculture. The level of IL-6 in PC-3 cells was significantly higher ($P<0.001$) under contact coculture conditions than in PC-3 cells under bilayer coculture conditions, whereas the level of IL-1β was not significantly different between the two coculture conditions (Figure 3B). The level of C3 in PC-3 cells was below the limits of detection under both bilayer and contact coculture conditions. Expression of COX-2 was determined by western blotting. The expression level of COX-2 was higher in PC-3 cells under contact coculture conditions than under bilayer coculture conditions (Figure 3C). Expression of COX-2 in the osteolytic bone metastasis model was also examined using immunohistochemistry. PC-3 cells formed solid tumour within the bone microenvironment in this tumour model, and strongly expressed COX-2 at the periphery of the tumour adjacent to the bone (Figure 3D, left). The close proximity of PC-3 cells to osteoblasts suggesting direct cancer-cell-osteoblast

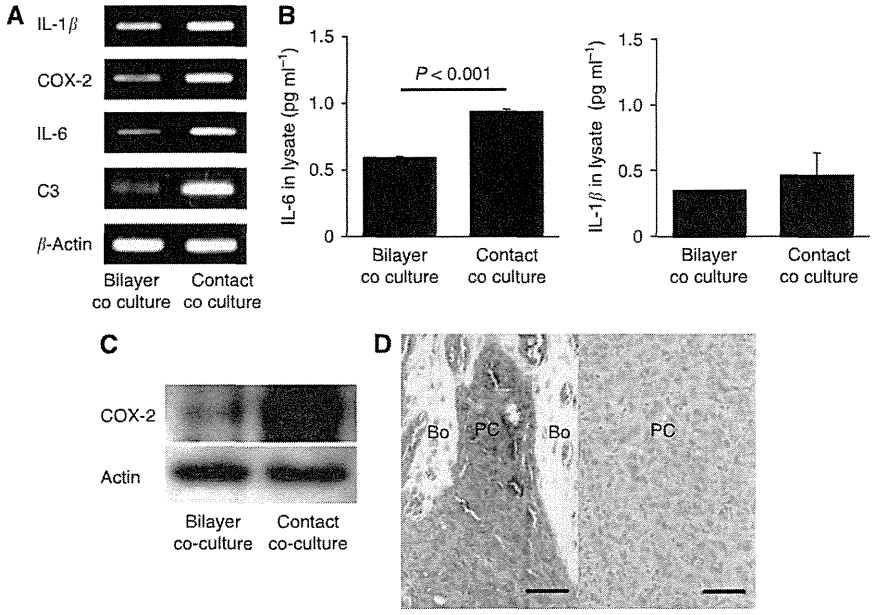

Figure 3 Analysis of IL-1β, COX-2, IL-6 and C3 expression in PC3 cells cocultured with hFOB1.19 cells. (**A**) The mRNA expression of the four osteoclastogenesis-related genes, IL-1β, COX-2, IL-6 and C3, in PC-3 cells following coculture under contact and bilayer conditions, was analysed using RT–PCR. Consistent with the cDNA microarray results, these genes were upregulated in contact cocultured PC-3 cells compared with bilayer cocultured cells. The primers used for RT–PCR are shown in Table 1. (**B**) Measurement of IL-6 and IL-1β levels in PC-3 cells using ELISA. The level of IL-6 was significantly higher ($P<0.001$) in PC-3 cells under contact coculture conditions than under bilayer coculture conditions, whereas IL-1β levels did not significantly differ between the two coculture conditions. ELISA was performed using a PC-3 cell lysate. (**C**) Analysis of COX-2 expression in PC-3 cells by western blotting. Expression of COX-2 was higher in PC-3 cells under contact coculture conditions than under bilayer coculture conditions. (**D**) Immunohistochemical analysis of COX-2 expression in an osteolytic bone metastasis model. Left: Strong expression of COX-2 in PC-3 cells adjacent to the bone. The close proximity of PC-3 cells to osteoblasts suggesting direct cancer-cell-osteoblast contact was observed in this area. Right: very low expression of COX-2 in PC-3 cells distant from the bone. Bo, bone; PC, prostate cancer cells. Scale = 50 μm.

contact was locally observed in this area. In contrast, in tumour areas that were distant from the bone, COX-2 expression was very low (Figure 3D, right). These results suggest that COX-2 expression in osteolytic prostate cancer cells correlates with physical contact between the cancer cells and osteoblasts in the bone microenvironment.

In vitro osteoclastogenesis

To examine the effect of physical contact between osteolytic cancer cells and osteoblasts on osteoclastogenic activity of cancer cells, an *in vitro* osteoclastogenesis assay was performed. In this assay, PC-3 cells that had been grown under contact or bilayer coculture conditions were lysed, and this lysate was then incubated with adherent bone marrow cells in the presence of RANKL and M-CSF for 10 days. The cells were then fixed and differentiated osteoclasts were detected by microscopic observation of TRAP staining. As shown in Figure 4, treatment with a cell lysate from PC-3 cells cocultured with hFOB1.19 cells under bilayer and contact conditions resulted in 20 ± 3 and 31 ± 7 TRAP-positive cells per field, respectively. The difference in number between the two culture conditions was statistically significant ($P<0.005$). These results suggest that the osteoclastogenic activity of osteolytic prostate cancer cells is enhanced by physical contact with osteoblasts.

N-cadherin and cadherin-11 neutralisation assay

We hypothesized that upregulation of osteoclastogenesis-related genes in PC-3 cells in contact cocultures may be induced by adhesion molecules that mediate interactions between PC-3 and hFOB1.19 cells. Both N-cadherin and cadherin-11 are overexpressed in osteoblasts (Marie, 2002; Mbalaviele *et al*, 2006) and prostate cancer cells (Tomita *et al*, 2000; Chu *et al*, 2008) and are considered to have an important role in bone metastasis of prostate cancer. We therefore determined if these cadherins might have a role in the upregulation of osteoclastogenesis-related genes in PC-3 cells under contact coculture conditions. For this purpose, we assayed if neutralisation of these cadherins using specific N-cadherin and cadherin-11 neutralising antibodies might inhibit the observed upregulation of these genes in PC-3 cells. We first confirmed that N-cadherin and cadherin-11 are expressed in both hFOB1.19 and PC-3 cells using RT–PCR (Figure 5A). Following pretreatment of hFOB1.19 cells with the cadherin-11 neutralising antibody, the upregulation of COX-2 and C3 mRNA that occurs in PC-3 cells under contact coculture conditions was inhibited. The ratio in level of COX-2 and C3 in anti-cadherin-11 antibody-treated cells to that in control antibody-treated cells were 0.49 and 0.60, respectively. In contrast, the upregulation of IL-1β and IL-6 mRNAs was not. Inversely, pretreatment with the N-cadherin-neutralising antibody further increased the upregulation of COX-2 mRNA. The ratio in level of COX-2 in anti-N-cadherin antibody-treated cells to that in control antibody-treated cells was 1.70 (Figure 5B). These results suggest that upregulation of osteoclastogenesis-related genes in PC-3 cells under contact coculture conditions is, at least in part, associated with both N-cadherin and cadherin-11.

DISCUSSION

In this study, we have shown that physical contact between osteolytic prostate cancer cells and osteoblasts may upregulate the expression of osteoclastogenesis-related genes in prostate cancer

cells, and enhance osteoclastogenesis. Microarray analysis of genes that were only expressed under contact coculture conditions and not under bilayer conditions, were considered to be specifically induced by physical contact between prostate cancer cells and osteoblasts.

We identified eight upregulated genes and one downregulated gene in PC-3 cells that were regulated only under contact coculture conditions. Interaction between cancer cells and osteoblasts has been previously studied using *in vitro* coculture systems in which conditioned medium or cell culture inserts have been employed. The results of these types of studies only reflect the effects of soluble factors and not of direct cell–cell contact. In our study, we did not detect any genes that were differentially expressed because of coculture of PC-3 cells and osteoblasts under bilayer conditions, where the PC-3 cells are only exposed to soluble factors produced by the osteoblasts. These results suggest that the contact coculture system may be useful for understanding the molecular mechanisms of interaction between prostate cancer cells and osteoblasts and for the detection of new molecular targets for the treatment of bone metastasis. Wang *et al* previously analysed gene expression in a contact coculture of PC-3 cells and rat bone marrow stromal cells. They detected 18 genes in PC-3 cells and 10 genes in bone marrow stromal cells, expression of which was regulated only in the physical contact coculture system (Wang *et al*, 2006). However, the regulated genes that they detected did not overlap with the genes that were regulated in our coculture system, indicating that osteoblasts and bone marrow stromal cells have different roles in prostate cancer bone metastasis.

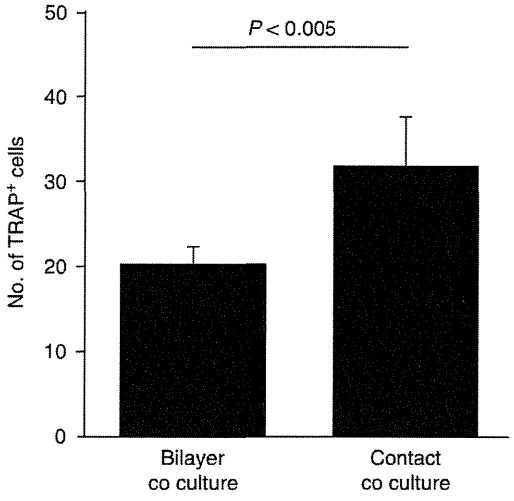

Figure 4 Osteoclastogenic activity of PC-3 cells cocultured with hFOB1.19 cells. The effect of addition of a cell lysate from PC-3 cells, grown under contact or bilayer coculture conditions, on osteoclastogenesis of bone marrow cells in an *in vitro* osteoclastogenesis assay, was determined by microscopic analysis of the number of tartrate-resistant acid phosphatase (TRAP) cells. The number of TRAP-positive cells in more than five microscopic fields was counted (× 200 magnification). Osteoclastogenesis was significantly enhanced by the cell lysate of PC-3 cells grown under contact coculture conditions compared with osteoclastogenesis with a lysate of cells grown under bilayer coculture conditions ($P < 0.005$). Data are representative of two separate experiments.

Four of the eight genes that we found to be upregulated in PC-3 cells under contact coculture conditions, that is, IL-1β, COX-2, IL-6 and C3 have already been reported to participate in osteoclastogenesis (Mangham *et al*, 1993; Sato *et al*, 1993; García-Moreno *et al*, 2002; Roodman, 2004; Liu *et al*, 2005; Singh *et al*, 2007; Bussard *et al*, 2008).

Cyclooxygenase-2 is an inducible prostaglandin synthesis enzyme, and is indirectly involved in bone resorption and osteoclastogenesis through prostaglandin E_2 (PGE_2) (Akatsu *et al*, 1989; Ohshiba *et al*, 2003). The expression of COX-2 is upregulated in many cancers. The product of COX-2, prostaglandin H_2, is converted by PGE_2 synthase into PGE_2, which can stimulate cancer progression (Menter *et al*, 2010). Cyclooxygenase-2 is overexpressed in primary prostate cancer with metastatic potential and its expression is associated with death from prostate carcinoma (Richardsen *et al*, 2010). Previously we have shown that neutralisation of PGE_2 using a soluble E-prostanoid receptor 2, inhibits the growth of PC-3 cells and tumour-induced osteoclastogenesis in a mouse model of bone metastasis (Takahashi *et al*, 2008).

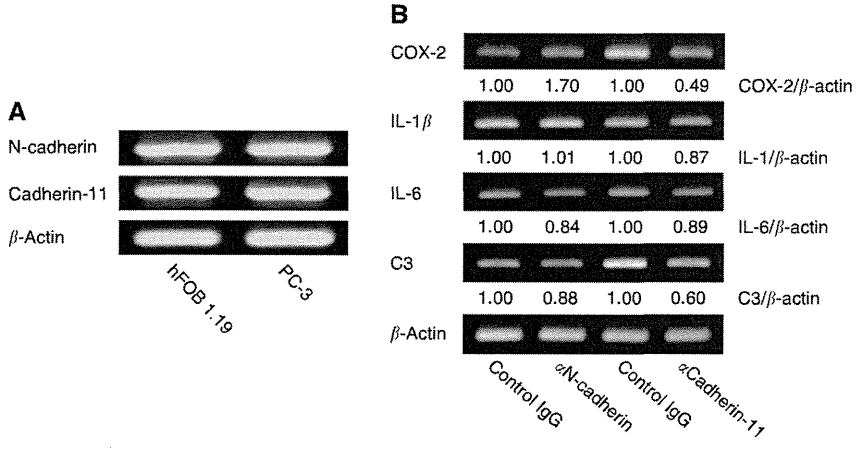

Figure 5 Effect of the blockade of N-cadherin- and cadherin-11-dependent cell adhesion between PC-3 and hFOB1.19 cells. (**A**) Confirmation of N-cadherin and cadherin-11 expression in both PC-3 cells and hFOB1.19 cells using RT–PCR. (**B**) Effects of N-cadherin or cadherin-11 neutralising antibodies on osteoclastogenesis-related gene expression in PC-3 cells under contact coculture conditions. The hFOB1.19 cells were pretreated with N-cadherin- or cadherin-11-neutralising antibodies for 30 min at 37°C, and then contact coculture with PC-3 cells was initiated. After 48 h, RNA was extracted from sorted PC-3 cells and was used as a template for RT–PCR to analyze the expression of the indicated osteoclastogenic genes. Signal intensities of each band were quantified by using NIHimage 1.62 software and normalised by that of β-actin. Data are representative of two separate experiments. The cadherin-11 neutralising antibody inhibited the upregulation of COX-2 and C3 mRNA, whereas the N-cadherin neutralising antibody further induced the upregulation of COX-2 mRNA.

Thus, our microarray results, that COX-2 expression is only upregulated in osteolytic PC-3 cells and not in osteoblastic MDA-PCa 2b cells, is consistent with the evidence that COX-2 and PGE_2 are key molecules for osteolytic bone metastasis. Furthermore, immunohistochemical analysis of an osteolytic bone metastasis model showed that COX-2 is strongly expressed in PC-3 cells that are adjacent to the bone and are locally in contact with osteoblasts, and is weakly expressed in PC-3 cells that are distant from the bone. These results suggest that the contact and bilayer coculture system may mimic the *in vivo* situation of metastatic cancer cells adjacent to and distant from the bone, respectively.

Interleukin-6 is a mediator of PGE_2-induced suppression of osteoprotegerin production by osteoblasts and enhances osteoclast differentiation (Liu *et al*, 2005). Interleukin-6 and the IL-6 receptor have been identified in human prostate carcinoma (Siegsmund *et al*, 1994) and IL-6 acts as an autocrine and paracrine growth factor in androgen-refractory prostate cancer cells including PC-3 cells (Chung *et al*, 1999). Immunohistochemical investigation of prostate cancer metastases and xenografts showed that IL-6 is expressed in the majority of prostate cancer bone metastases and to a lesser extent in prostate cancer soft tissue metastases (Morrissey *et al*, 2010). Our data is consistent with the results of these reports.

IL-1β has been found to increase the formation as well as the resorptive capacity of osteoclasts in culture (Trebec-Reynolds *et al*, 2010), and can induce IL-8 production in prostate cancer cells, which promotes prostate cancer cell proliferation and migration (Tsai *et al*, 2009). Although we confirmed the cDNA microarray result of IL-1β mRNA upregulation using RT-PCR, the protein level of IL-1β in PC-3 cell lysates was not significantly different under bilayer and contact coculture conditions. The reason for this discrepancy is unknown, but it may involve posttranscriptional or posttranslational regulatory mechanisms.

C3 participates in osteoclast development by potentiating M-CSF-dependent proliferation of bone marrow cells and induction of osteoclast differentiation (Sato *et al*, 1993). The concentrations of C3 in prostatic fluid are significantly greater in patients with prostate cancer than those with benign prostate hyperplasia. However, in our study it was not possible to determine differences in the level of C3 protein between PC-3 cells under bilayer and contact coculture conditions, as the C3 protein level was below the limits of detection of ELISA analysis.

The roles of other four upregulated genes, that is, tumour necrosis factor, alpha-induced protein 6, fatty acid binding protein 4, tripartite motif-containing 31, small Cajal body-specific RNA 6 on chromosome 2 and one downregulated gene, that is, secreted protein acidic and rich in cysteine (SPARC; also known as osteonectin) on osteoclastogenesis and bone metastasis must be clarified in future studies. Especially, SPARC has been assumed to be important in human prostate cancer bone metastasis as a major bone-derived chemoattractant for prostate cancer cells (Jacob *et al*, 1999). On the other hand, downregulation of endogenous SPARC by small interference RNA accelerates prostate cancer cell-line proliferation and matrix invasiveness (Said *et al*, 2009). Participation of SPARC in osteoclastogenesis is unclear. However, SPARC stimulates the synthesis of osteoprotegerin, a physiological inhibitor of osteoclastogenesis, in human periodontal ligament cells (Fujita *et al*, 2002).

We showed that PC-3 cells that were cocultured with hFOB1.19 cells under contact conditions had significantly higher osteoclastogenic activity in an *in vitro* osteoclastogenesis assay than cells cultured under bilayer conditions. On the basis of the observed protein expression levels, it would appear that COX-2 and IL-6, rather than IL-1β and C3, are the major molecules that influence this enhancement of osteoclastogenesis in the contact coculture system.

Cell adhesion molecules have been suggested to have a primary role in the interactions between tumour cells and host environment (Michigami *et al*, 2000; Cowin *et al*, 2005). In particular, cadherins have been proposed to function as tumour promoter factors during cancer invasion and organ preferential metastasis (Pishvaian *et al*, 1999; Gravdal *et al*, 2007). N-cadherin and cadherin-11 are transmembrane calcium-dependent and homophilic cell-cell adhesion molecules. These molecules have been detected in prostate cancers (Tomita *et al*, 2000) and in osteoblasts (Cheng *et al*, 1998; Mbalaviele *et al*, 2006) and have been reported to be implicated in cancer invasion and human osteoblast differentiation (Kii *et al*, 2004; Chu *et al*, 2008). These finding led us to hypothesize that N-cadherin and cadherin-11 may participate in the upregulation of osteoclastogenesis-related genes that was mediated by physical contact between PC-3 and hFOB1.19 cells. Consistent with previous studies, we found that N-cadherin and cadherin-11 were both expressed in PC-3 and hFOB1.19 cells. Pre-treatment of hFOB1.19 cells with cadherin-11-neutralising antibody before initiation of the coculture inhibited the upregulation of COX-2 and C3 mRNA that was induced in PC-3 cells under contact coculture conditions. In contrast, pre-treatment with N-cadherin neutralising antibody upregulated COX-2 mRNA in PC-3 cells under contact coculture conditions. These data suggest that cadherin-11 and N-cadherin are involved in the process of osteoclastogenesis that is induced by physical contact between osteolytic prostate cancer cells and osteoblasts.

There is a great deal of evidence indicating that interaction between prostate cancer cells and osteoblasts has an important role in the survival and growth of metastatic cancer cells in a bone microenvironment (Logothetis and Lin, 2005; Morrissey *et al*, 2010). Physical contact between cancer cells and osteoblasts has been suggested to be involved in these processes. However, when we histologically analysed osteolytic tumours that were produced by intratibial injection of PC-3 cells into nude mice, the bone surfaces facing the tumours were extensively lysed by osteoclasts. Although residual osteoblasts and the close proximity of PC-3 cells to osteoblasts suggesting direct cancer-cell-osteoblast contact was observed in some areas (Figure 1A), the question remained whether this type of cell-cell contact is common in human cases of bone metastases or not. However, in all 37 autopsy cases with osteoblastic or osteolytic bone metastases that we reviewed, the close proximity of cancer cells to osteoblasts suggesting direct cancer-cell-osteoblast contact was observed to varying extents. Although we could not confirm direct cancer-cell-osteoblast contact by electron microscopy, these results suggest that direct cancer-cell-osteoblast contact is common, at least in advanced bone metastases. In future studies, it must be clarified whether metastatic cancer cells physically contact with osteoblasts in early bone metastasis, either as a single cell or as a small focus of cells.

In this study, we have shown that direct metastatic cancer-cell-osteoblast contact likely to be a common event in cases with advanced bone metastases. We further show that physical contact between osteolytic prostate cancer cells and osteoblasts may enhance the osteoclastogenic activity of prostate cancer cells by inducing upregulation of the gene expression of specific osteoclastogenesis-related genes. Additionally, this process is, at least in part, cadherin-11 dependent. These data provide evidence to support the design of new therapies of prostate cancer bone metastasis that target direct cancer-cell-osteoblast contact.

ACKNOWLEDGEMENTS

We thank Megumi Kume and Hitomi Umemoto for technical assistance. This work was supported by a Grant-in-Aid for Scientific Research (No. 21390442 to H.K.) provided by the Ministry of Education, Culture, Sports, Science and Technology, Japan, and was partly supported by an Extramural Collaborative Research Grant from the Cancer Research Institute, Kanazawa University.

REFERENCES

Akatsu T, Takahashi N, Debari K, Morita I, Murota S, Nagata N, Takatani O, Suda T (1989) Prostaglandins promote osteoclastlike cell formation by a mechanism involving cyclic adenosine 3′,5′-monophosphate in mouse bone marrow cell cultures. *J Bone Miner Res* 4(1): 29–35

Bubendorf L, Schopfer A, Wagner U, Sauter G, Moch H, Willi N, Gasser TC, Mihatsch MJ (2000) Metastatic patterns of prostate cancer: an autopsy study of 1589 patients. *Human Pathol* 31(5): 578–583

Bussard KM, Gay CV, Mastro AM (2008) The bone microenvironment in metastasis; what is special about bone? Review. *Cancer Metastasis Rev* 27(1): 41–55

Charhon SA, Chapuy MC, Delvin EE, Valentin-Opran A, Edouard CM, Meunier PJ (1983) Histomorphometric analysis of sclerotic bone metastases from prostatic carcinoma special reference to osteomalacia. *Cancer* 51(5): 918–924

Cheng SL, Lecanda F, Davidson MK, Warlow PM, Zhang SF, Zhang L, Suzuki S, St John T, Civitelli R (1998) Human osteoblasts express a repertoire of cadherins, which are critical for BMP-2-induced osteogenic differentiation. *J Bone Miner Res* 13(4): 633–644

Cheville JC, Tindall D, Boelter C, Jenkins R, Lohse CM, Pankratz VS, Sebo TJ, Davis B, Blute ML (2002) Metastatic prostate carcinoma to bone: clinical and pathologic features associated with cancer-specific survival. *Cancer* 95(5): 1028–1036

Chu K, Cheng CJ, Ye X, Lee YC, Zurita AJ, Chen DT, Yu-Lee LY, Zhang S, Yeh ET, Hu MC, Logothetis CJ, Lin SH (2008) Cadherin-11 promotes the metastasis of prostate cancer cells to bone. *Mol Cancer Res* 6(8): 1259–1267

Chung TD, Yu JJ, Spiotto MT, Bartkowski M, Simons JW (1999) Characterization of the role of IL-6 in the progression of prostate cancer. *Prostate* 38(3): 199–207

Cowin P, Rowlands TM, Hatsell SJ (2005) Cadherins and catenins in breast cancer. *Curr Opin Cell Biol* 17(5): 499–508

Fizazi K, Yang J, Peleg S, Sikes CR, Kreimann EL, Daliani D, Olive M, Raymond KA, Janus TJ, Logothetis CJ, Karsenty G, Navone NM (2003) Prostate cancer cells-osteoblast interaction shifts expression of growth/survival-related genes in prostate cancer and reduces expression of osteoprotegerin in osteoblasts. *Clin Cancer Res* 9(7): 2587–2597

Fujita T, Shiba H, Sakata M, Uchida Y, Nakamura S, Kurihara H (2002) SPARC stimulates the synthesis of OPG/OCIF, MMP-2 and DNA in human periodontal ligament cells. *J Oral Pathol Med* 31(6): 345–352

García-Moreno C, Méndez-Dávila C, de La Piedra C, Castro-Errecaborde NA, Traba ML (2002) Human prostatic carcinoma cells produce an increase in the synthesis of interleukin-6 by human osteoblasts. *Prostate* 50(4): 241–246

Gravdal K, Halvorsen OJ, Haukaas SA, Akslen LA (2007) A switch from E-cadherin to N-cadherin expression indicates epithelial to mesenchymal transition and is of strong and independent importance for the progress of prostate cancer. *Clin Cancer Res* 13(23): 7003–7011

Harris SA, Enger RJ, Riggs BL, Spelsberg TC (1995) Development and characterization of a conditionally immortalized human fetal osteoblastic cell line. *J Bone Miner Res* 10(2): 178–186

Hullinger TG, Taichman RS, Linseman DA, Somerman MJ (2000) Secretory products from PC-3 and MCF-7 tumor cell lines upregulate osteopontin in MC3T3-E1 cells. *J Cell Biochem* 78(4): 607–616

Jacob K, Webber M, Benayahu D, Kleinman HK (1999) Osteonectin promotes prostate cancer cell migration and invasion: a possible mechanism for metastasis to bone. *Cancer Res* 59(17): 4453–4457

Jemal A, Siegel R, Ward E, Hao Y, Xu J, Murray T, Thun MJ (2008) Cancer statistics, 2008. *CA Cancer J Clin* 58(2): 71–96

Kido J, Yamauchi N, Ohishi K, Kataoka M, Nishikawa S, Nakamura T, Kadono H, Ikedo D, Ueno A, Nonomura N, Okuyama A, Nagata T (1997) Inhibition of osteoblastic cell differentiation by conditioned medium derived from the human prostatic cancer cell line PC-3 *in vitro*. *J Cell Biochem* 67(2): 248–256

Kii I, Amizuka N, Shimomura J, Saga Y, Kudo A (2004) Cell-cell interaction mediated by cadherin-11 directly regulates the differentiation of mesenchymal cells into the cells of the osteo-lineage and the chondro-lineage. *J Bone Miner Res* 19(11): 1840–1849

Lang SH, Miller WR, Habib FK (1995) Stimulation of human prostate cancer cell lines by factors present in human osteoblast-like cells but not in bone marrow. *Prostate* 27(5): 287–293

Liu XH, Kirschenbaum A, Yao S, Levine AC (2005) Cross-talk between the interleukin-6 and prostaglandin E(2) signaling systems results in enhancement of osteoclastogenesi. *Endocrinology* 146(4): 1991–1998

Logothetis CJ, Lin SH (2005) Osteoblasts in prostate cancer metastasis to bone. *Nat Rev Cancer* 5(1): 21–28

Mangham DC, Scoones DJ, Drayson MT (1993) Complement and the recruitment of mononuclear osteoclasts. *J Clin Pathol* 46(6): 517–521

Marie PJ (2002) Role of N-cadherin in bone formation. *J Cell Physiol* 190(3): 297–305

Martínez J, Silva S, Santibanez JF (1996) Prostate-derived soluble factors block osteoblast differentiation in culture. *J Cell Biochem* 61(1): 18–25

Mbalaviele G, Shin CS, Civitelli R (2006) Cell-cell adhesion and signaling through cadherins: connecting bone cells in their microenvironment. *J Bone Miner Res* 21(12): 1821–1827

Menter DG, Schilsky RL, DuBois RN (2010) Cyclooxygenase-2 and cancer treatment: understanding the risk should be worth the reward. *Clin Cancer Res* 16(5): 1384–1390

Michigami T, Shimizu N, Williams PJ, Niewolna M, Dallas SL, Mundy GR, Yoneda T (2000) Cell-cell contact between marrow stromal cells and myeloma cells via VCAM-1 and alpha(4)beta(1)-integrin enhances production of osteoclast-stimulating activity. *Blood* 96(5): 1953–1960

Morrissey C, Lai JS, Brown LG, Wang YC, Roudier MP, Coleman IM, Gulati R, Vakar-Lopez F, True LD, Corey E, Nelson PS, Vessella RL (2010) The expression of osteoclastogenesis-associated factors and osteoblast response to osteolytic prostate cancer cells. *Prostate* 70(4): 412–424

Mundy GR (2002) Metastasis to bone: causes, consequences and therapeutic opportunities. *Nat Rev Cancer* 2(8): 584–593

Ohshiba T, Miyaura C, Ito A (2003) Role of prostaglandin E produced by osteoblasts in osteolysis due to bone metastasis. *Biochem Biophys Res Commun* 300(4): 957–964

Pishvaian MJ, Feltes CM, Thompson P, Bussemakers MJ, Schalken JA, Byers SW (1999) Cadherin-11 is expressed in invasive breast cancer cell lines. *Cancer Res* 59(4): 947–952

Richardsen E, Uglehus RD, Due J, Busch C, Busund LT (2010) COX-2 is overexpressed in primary prostate cancer with metastatic potential and may predict survival. A comparison study between COX-2, TGF-beta, IL-10 and Ki67. *Cancer Epidemiol* 34(3): 316–322

Roodman GD (2004) Mechanisms of bone metastasis. Review. *N Engl J Med* 350(16): 1655–1664

Roudier MP, True LD, Higano CS, Vesselle H, Ellis W, Lange P, Vessella RL (2003) Phenotypic heterogeneity of end-stage prostate carcinoma metastatic to bone. *Hum Pathol* 34(7): 646–653

Said N, Frierson Jr HF, Chernauskas D, Conaway M, Motamed K, Theodorescu D (2009) The role of SPARC in the TRAMP model of prostate carcinogenesis and progression. *Oncogene* 28(39): 3487–3498

Sato T, Abe E, Jin CH, Hong MH, Katagiri T, Kinoshita T, Amizuka N, Ozawa H, Suda T (1993) The biological roles of the third component of complement in osteoclast formation. *Endocrinology* 133(1): 397–404

Siegsmund MJ, Yamazaki H, Pastan I (1994) Interleukin 6 receptor mRNA in prostate carcinomas and benign prostate hyperplasia. *J Urol* 151(5): 1396–1399

Sim HG, Cheng CW (2005) Changing demography of prostate cancer in Asia. *Eur J Cancer* 41(6): 834–845

Singh B, Berry JA, Shoher A, Ayers GD, Wei C, Lucci A (2007) COX-2 involvement in breast cancer metastasis to bone. *Oncogene* 26(26): 3789–3796

Takahashi T, Uehara H, Bando Y, Izumi K (2008) Soluble EP2 neutralizes prostaglandin E2-induced cell signaling and inhibits osteolytic tumor growth. *Mol Cancer Ther* 7(9): 2807–2816

Tomita K, van Bokhoven A, van Leenders GJ, Ruijter ET, Jansen CF, Bussemakers MJ, Schalken JA (2000) Cadherin switching in human prostate cancer progression. *Cancer Res* 60(13): 3650–3654

Trebec-Reynolds DP, Voronov I, Heersche JN, Manolson MF (2010) IL-1alpha and IL-1beta have different effects on formation and activity of large osteoclasts. *J Cell Biochem* 109(5): 975–982

Tsai CY, Lee TS, Kou YR, Wu YL (2009) Glucosamine inhibits IL-1beta-mediated IL-8 production in prostate cancer cells by MAPK attenuation. *J Cell Biochem* 108(2): 489–498

Uehara H, Kim SJ, Karashima T, Shepherd DL, Fan D, Tsan R, Killion JJ, Logothetis C, Mathew P, Fidler IJ (2003) Effects of blocking platelet-derived growth factor-receptor signaling in a mouse model of experimental prostate cancer bone metastases. *J Natl Cancer Inst* 95(6): 458–470

Wang J, Levenson AS, Satcher RL (2006) Identification of a unique set of genes altered during cell-cell contact in an *in vitro* model of prostate cancer bone metastasis. *Int J Mol Med* 17(5): 849–856

Yin JJ, Pollock CB, Kelly K (2005) Mechanisms of cancer metastasis to the bone. *Cell Research* 15(1): 57–62

A multi-institutional phase II study of combination chemotherapy with S-1 plus cisplatin in patients with advanced non-small cell lung cancer

HIDEKI TOMIMOTO[1], MASAKI HANIBUCHI[2], FUMITAKA OGUSHI[3], YOSHIO OKANO[4], TSUTOMU SHINOHARA[3], HIROYUKI DOI[4], AKIYOSHI YAMAMOTO[5], EIJI TAKEUCHI[6], AKIHIKO YAMAMOTO[7], MASAHIKO AZUMA[2], HIROYA TADA[8], TAKANORI KANEMATSU[2], SOJI KAKIUCHI[1], HISATSUGU GOTO[2], SEIJI YANO[2], YASUHIKO NISHIOKA[2] and SABURO SONE[1,2]

Departments of [1]Medical Oncology, [2]Respiratory Medicine and Rheumatology, Institute of Health Biosciences, University of Tokushima Graduate School, Tokushima 770-8503; [3]Department of Respiratory Medicine, National Hospital Organization, Kochi National Hospital, Kochi 780-8077; [4]Department of Respiratory Medicine and Allergology, Kochi Health Sciences Center, Kochi 781-8555; [5]Division of Respirology, Takamatsu Red Cross Hospital, Takamatsu 760-0017; [6]Department of Internal Medicine, Kochi Red Cross Hospital, Kochi 780-8562; [7]Division of Respirology, Matsuyama Red Cross Hospital, Matsuyama 790-8524; [8]Department of Respiratory Medicine, National Hospital Organization, Zentsuji National Hospital, Zentsuji 765-8507, Japan

Received September 22, 2010; Accepted December 23, 2010

DOI: 10.3892/ol.2011.266

Abstract. S-1 is an oral anticancer fluoropyrimidine agent designed to elevate anticancer activity with a decrease in gastrointestinal toxicity. We conducted a phase II study to evaluate the efficacy and safety of combination chemotherapy with S-1 plus cisplatin in patients with advanced non-small cell lung cancer (NSCLC). Chemotherapy-naïve patients were treated with S-1 administered orally at 40 mg/m^2 twice a day for 21 consecutive days, and cisplatin (60 mg/m^2) infused intravenously on day 8, repeated every 5 weeks. Of the 44 patients enrolled in the study, 40 were assessable for efficacy and safety. The median number of cycles administered was 3 (range 1-9 cycles). Among the 40 assessable patients, 7 partial responses were observed, with an overall response rate (RR) of 17.5% [95% confidence interval (CI), 5.2-29.8]. Patients with squamous cell carcinoma showed a significantly higher RR (55.5%) than those with adenocarcinoma (9.1%) or other types of NSCLC (0%). The median progression-free survival was 4.3 months (95% CI, 3.4-4.9), the median survival time was 17.9 months (95% CI, 15.0-20.8), and the 1- and 2-year survival rates were 63.3 and 27.3%, respectively. Major grade 3-4 hematologic toxicities were leukocytopenia (7.5%), neutropenia (5.0%), anemia (15.0%) and thrombocytopenia (2.5%). No grade 4 non-hematologic toxicity or treatment-related death occurred. These results suggest that combination chemotherapy with S-1 plus cisplatin is a promising therapeutic candidate for patients with advanced NSCLC, particularly squamous cell carcinoma.

Correspondence to: Professor Saburo Sone, Department of Respiratory Medicine and Rheumatology, Institute of Health Biosciences, University of Tokushima Graduate School, 3-18-15 Kuramoto-cho, Tokushima, 770-8503, Japan
E-mail: ssone@clin.med.tokushima-u.ac.jp

Abbreviations: NSCLC, non-small cell lung cancer; 5-FU, 5-fluorouracil; CDHP, 5-chloro-2,4-dihydroxypyridine; RR, response rate; MST, median survival time; CDDP, cisplatin; ECOG, Eastern Cooperative Oncology Group; BSA, body surface area; PFS, progression-free survival; 95% CI, 95% confidence interval; PR, partial response; SD, stable disease; PD, progressive disease; TP, thymidine phosphorylase; DPD, dihydropyrimidine dehydrogenase

Key words: combination chemotherapy, S-1, cisplatin, non-small cell lung cancer

Introduction

Lung cancer is the leading cause of malignancy-related death worldwide, with a mortality rate of 80-90% (1). Among patients with lung cancer, 85% are diagnosed as having non-small cell lung cancer (NSCLC). Despite efforts, innovations, and progress in the diagnosis and treatment of these patients, patient survival at 5 years after diagnosis is only 15% (1). Therefore, novel therapeutic strategies to improve the outcome of patients with NSCLC are urgently required.

S-1 is an oral anticancer fluoropyrimidine agent comprising the 5-fluorouracil (5-FU) prodrug tegafur and two enzyme inhibitors, 5-chloro-2, 4-dihydroxypyridine (CDHP) and potassium oxonate (2,3). Since CDHP inhibits dihydropyrimidine dehydrogenase activity and potassium oxonate suppresses pyrimidine phosphoribosyl transferase activity, oral S-1 administration generates a higher concentration of 5-FU than a protracted intravenous injection of 5-FU, without increasing the incidence

of adverse events in the gastrointestinal tract (4-6). In a phase II trial, involving monotherapy with S-1 at 80 mg/m^2/day for 28 days followed by a 2-week rest period in chemotherapy-naïve patients with advanced NSCLC, the overall response rate (RR) was 22.0% and the median survival time (MST) was 10.2 months (7). Moreover, two phase II trials of S-1 plus cisplatin (CDDP) for advanced NSCLC (stage IIIB, without any indication for radiotherapy, or stage IV) yielded RRs of 32.7-47% and MSTs of 11-16 months with a mild toxicity profile (8,9). Recent evidence has indicated favorable efficacy of S-1 in combination with chemotherapeutic agents, with the exception of CDDP, for advanced NSCLC (10,11). Although the results suggest the efficacy of combinations of S-1 with other chemotherapeutic agents, the therapeutic efficacy and safety of combination chemotherapy with S-1 plus CDDP in patients with advanced NSCLC have yet to be elucidated.

In the present study, a phase II study of combination chemotherapy with S-1 (40 mg/m^2 twice a day on days 1-21 followed by a 2-week rest) and CDDP (60 mg/m^2 on day 8, every 5 weeks) was conducted in patients with advanced NSCLC, and the efficacy and safety of this regimen were determined. The MST of 17.9 months occurred over a longer period of time, and the incidence of adverse events was lower than that for standard NSCLC chemotherapy. Furthermore, an overall RR in patients with squamous cell carcinoma was statistically superior compared with that in patients with adenocarcinoma or other types of NSCLC. These findings suggest that combination chemotherapy with S-1 plus CDDP is a promising therapeutic candidate for patients with advanced NSCLC, particularly squamous cell carcinoma.

Patients and methods

Patient eligibility. Patients were eligible for this phase II trial in the event that they were either cytologically or histologically confirmed to have NSCLC; were in stage IIIB, without any indication of radical thoracic radiotherapy, or stage IV; had measurable disease; received no prior treatment; were in the age range of 20-74 years; had an Eastern Cooperative Oncology Group (ECOG) performance status of 0 or 1; and had a projected life expectancy of at least 3 months. Other eligibility criteria for organ function included: leukocyte count 4000-12,000/μl, absolute granulocyte count ≥2000/μl, platelet count ≥100,000/μl, hemoglobin level ≥9 g/dl, serum bilirubin level ≤1.5 mg/dl, serum aspartate aminotransferase and alanine amino transferase levels ≤100 IU/l, alkaline phosphatase level of twice the upper limit or less, normal creatinine level, creatinine clearance rate of ≥60 ml/min, and arterial oxygen partial pressure of ≥60 Torr. Since S-1 is in tablet form, patients were required to be able to swallow. For staging, all 44 patients underwent a computed tomography scan of the thorax, including upper abdomen, and either a brain computed tomography scan or magnetic resonance imaging of the brain. A radioisotopic bone scan was also performed in the majority of the patients.

Exclusion criteria included pregnancy or serious concomitant disease, concomitant malignancy, pleural effusion requiring treatment, or symptomatic cerebral involvement. Written informed consent was obtained from all patients, and the protocol was approved by the Institutional Review Board of each of the participating institutions. On enrollment to the study, the eligibility of the patients was reviewed by the Central Administration Office at the Department of Respiratory Medicine and Rheumatology, University of Tokushima, Japan.

Treatment schedule. Oral administration of S-1 at 40 mg/m^2 occurred twice a day, after meals, on days 1-21. The actual dose of S-1 administration was selected as follows: in a patient with a body surface area (BSA) <1.25 m^2, 40 mg twice a day; BSA of 1.25 m^2 but <1.5 m^2, 50 mg twice a day; and BSA ≥1.5 m^2, 60 mg twice a day. CDDP (60 mg/m^2) was administered intravenously on day 8 when patients were hydrated by infusion of at least 2,500 ml. Administration of an antiemetic agent was permitted at the discretion of each patient's physician. The treatment regimen was repeated every 5 weeks until disease progression or unacceptable toxicity occurred. A leukocyte count of ≥3000/μl, an absolute granulocyte count of ≥1500/μl, a platelet count of ≥100,000/μl and the entry eligibility criteria regarding organ functions had to be achieved in order for the following cycle to commence. If these criteria were satisfied 4 weeks after day 1 of each cycle of chemotherapy, administration of the following cycle was allowed. The doses of S-1 were adjusted according to the degree of hematologic and non-hematologic toxicity. The dose was reduced by one level (20 mg per day) in patients with evidence of grade 4 hematologic toxicity or grade ≥3 non-hematologic toxicity during any cycle of administration. If recovery from such toxicities was confirmed at a reduced dose, administration at the reduced dose was continued. If a rest period of ≥3 weeks was required, the patient was withdrawn from the study.

Evaluation of response and toxicity. Eligible patients who received at least one course of S-1 plus CDDP were considered assessable for response and toxicity. Chest X-ray, complete blood count, and blood chemistry studies were repeated at least once a week. The response was assessed based on the computed tomography scan findings that had been used initially to define the extent of the tumor. The response was evaluated at the end of each treatment cycle in accordance with the Response Evaluation Criteria in Solid Tumors version 1.0. Adverse events were graded according to the National Cancer Institute Common Toxicity Criteria version 3.0.

Statistical analysis. The primary end point was RR; secondary end points included progression-free survival (PFS), overall survival and adverse events. PFS was defined as the time from registration to progression or death from any cause. Overall survival was defined as the time from registration to death from any cause or when the patient was last known to be alive. The minimum number of patients to be enrolled in this study was defined as 34, with the assumption that the 95% CI would be 30% under conditions giving an α error of 0.025 (one-sided) and a β error of 0.2, assuming an anticipated RR of 50%. Consequently, 40 patients were included to allow for patient dropout. The median PFS and MST were estimated by the Kaplan-Meier method of univariate analysis. The differences between categorized groups were compared by the one-way ANOVA test. All statistical tests were two-sided, and $p<0.05$ was considered to be statistically significant.

Table I. Patient characteristics.

No. of patients	40	
Age (years)		
Median (range)	64	(27-74)
Gender		
Male	32	(80.0%)
Female	8	(20.0%)
Performance status (ECOG)		
0	12	(30.0%)
1	28	(70.0%)
Stage		
IIIB	13	(32.5%)
IV	27	(67.5%)
Histology		
Adenocarcinoma	22	(55.0%)
Squamous cell carcinoma	9	(22.5%)
Others	9	(22.5%)

ECOG, Eastern Cooperative Oncology Group.

Results

Patient population. Between July 2005 and November 2008, 44 patients with advanced NSCLC from 7 institutions were enrolled in this study. Of the 44 patients, 40 were assessable for efficacy and safety. Two patients were excluded since they declined entry to the study after enrollment. Two other patients were considered not to be assessable as they were unable to receive any CDDP due to high fever and massive pleural effusion, respectively, after S-1 treatment had commenced. The clinical characteristics of the 40 assessable patients are shown in Table I. Patients included 32 males (80%) and 8 females (20%). The median age was 64 years (range 27-74). The patients had an ECOG performance status of 0 (12/40, 30%) or 1 (28/40, 70%). A total of 13 patients (32.5%) had stage IIIB and 27 (67.5%) had stage IV NSCLC. The predominant histological type was adenocarcinoma (55%), followed by squamous cell carcinoma (22.5%) and other types of NSCLC (22.5%).

Response and survival. No complete response (CR) was observed in the 40 patients, whereas 7 patients showed a partial response (PR), yielding an overall RR of 17.5% (95% CI 5.2-29.8). Stable disease (SD) was observed in 25 patients (62.5%). Thus, the disease control rate (PR+SD) was 80% (95% CI 67.1-92.9). Eight patients (20%) showed progressive disease (PD). Table II shows patient characteristics in relation to response. No statistically significant differences were noted in the RRs among gender and stages. Notably, the overall RR in patients with squamous cell carcinoma (55.5%) was statistically superior compared with the RR in patients with adenocarcinoma or other types of NSCLC (9.1%, p=0.012; 0.0%, p=0.009, respectively). The MST of the 40 assessable patients was 17.9 months (95% CI 15.0-20.8), and the 1- and 2-year survival rates were 63.3 and 27.3%, respectively (Fig. 1). As shown in Fig. 2, the median PFS was 4.3 months (95% CI 3.4-4.9). Exploratory analyses of the survival according to histological subtypes showed no significant differences in the MST and median PFS. The MSTs and median PFSs of patients with squamous cell carcinoma, adenocarcinoma and other types of NSCLC were 21.1 and 6.5 months, 17.9 and 4 months, and 14.5 and 4.2 months, respectively.

Adverse events. Table III shows the major adverse events in the 40 assessable patients during the entire treatment period. The hematological adverse events reaching grades 3-4 were anemia (15%), leukocytopenia (7.5%), neutropenia (5%) and thrombocytopenia (2.5%). Febrile neutropenia was observed in only one patient (2.5%). Grade 3 non-hematologic adverse events were anorexia (12.5%), nausea/vomiting (7.5%), infection (5%), general fatigue (2.5%) and gastric ulcer (2.5%). No cases

Table II. Patient characteristics in relation to the response.

		Response				
Characteristics	No. of patients	CR	PR	SD	PD	Response rate (%)
No. of patients	40	0	7	25	8	17.5
Gender						
Male	32	0	5	19	8	15.6
Female	8	0	2	6	0	25.0
Stage						
IIIB	13	0	2	8	3	15.4
IV	27	0	5	17	5	18.5
Histology						
Adenocarcinoma	22	0	2	15	5	9.1
Squamous cell carcinoma	9	0	5	3	1	55.5
Others	9	0	0	7	2	0.0

CR, complete response; PR, partial response; SD, stable disease; PD, progressive disease.

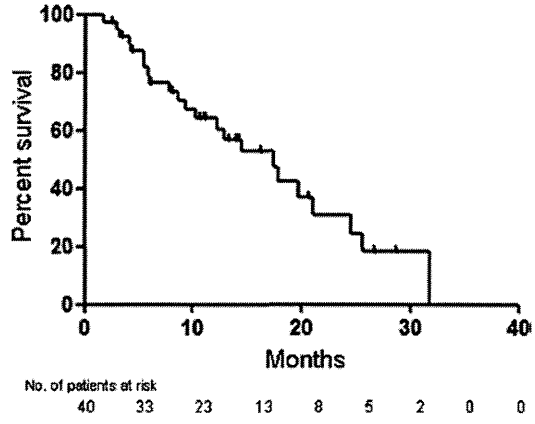

Figure 1. Overall survival of 40 assessable patients was calculated according to the Kaplan-Meier method. The median survival time was 17.9 months (95% CI 15.0-20.8), and the 1- and 2-year survival rates were 63.3 and 27.3%, respectively.

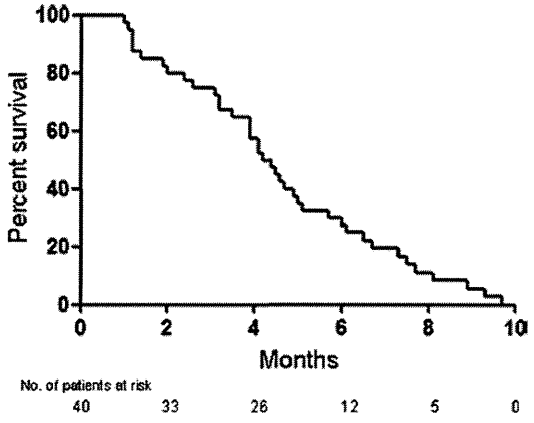

Figure 2. Progression-free survival of 40 assessable patients was calculated according to the Kaplan-Meier method. The median progression-free survival was 4.3 months (95% CI 3.4-4.9).

of grade 4 toxicity occurred. Moreover, no instance of irreversible toxicity or treatment-related death was noted.

Compliance. The median number of cycles administered was 3, with a range of 1-9 treatment cycles (1 cycle, 7 patients; 2 cycles, 9 patients; 3 cycles, 8 patients; 4 cycles, 12 patients; ≥5 cycles, 4 patients). The reasons for administration of only one cycle of treatment were PD in 5 patients and adverse events in 2 patients. A total of 122 cycles were administered to the 40 patients. Seven patients required temporary or permanent cessation in S-1 during the treatment courses due to adverse events, including myelosuppression in 4 patients, pulmonary toxicity in 2, and gastrointestinal toxicity in 1 patient. No dose reduction of S-1 was required in any of the 40 assessable patients. CDDP administration was disregarded in 4 patients due to myelosuppression, and the dose of CDDP was reduced in 1 patient due to gastrointestinal toxicity.

Discussion

The present study indicates that combination chemotherapy with S-1 plus CDDP may constitute an efficacious and well-tolerated therapeutic option for patients with treatment-naïve advanced NSCLC. The MST of 17.9 months occurred over a longer period of time, and the incidence of adverse events was lower than the values for the standard NSCLC chemotherapy. Consequently, combination chemotherapy with S-1 plus CDDP is a promising therapeutic candidate for patients with advanced NSCLC.

Table III. Hematologic and non-hematologic toxicities.

Adverse events	Grade			Grade 3-4
	2	3	4	(%)
Leukocytopenia	7	3	0	7.5
Neutropenia	6	2	0	5.0
Anemia	8	4	2	15.0
Thrombocytopenia	5	0	1	2.5
Liver disorder	4	0	0	0.0
Bilirubin	1	0	0	0.0
Creatinine	2	0	0	0.0
Hyponatremia	0	1	0	2.5
Infection	0	2	0	5.0
Anorexia	6	5	0	12.5
Nausea/vomiting	7	3	0	7.5
General fatigue	4	1	0	2.5
Gastric ulcer	0	1	0	2.5
Diarrhea	2	0	0	0.0
Constipation	1	0	0	0.0
Stomatitis	1	0	0	0.0
Desquamation	1	0	0	0.0
Fever	1	0	0	0.0

A phase II trial of combination chemotherapy with S-1 at 80 mg/m^2/day for 21 days and CDDP at 60 mg/m^2 on day 8 yielded a RR of 47.3% and a MST of 11 months (8). Ozawa *et al* also reported a phase II study of combination chemotherapy with S-1 at 80 mg/m^2/day for 21 days and weekly CDDP at 25 mg/m^2/week on days 7, 14 and 21, which yielded a RR of 23.1% and a MST of 13.4 months (9). Compared with the reported RRs and MSTs of 17-28% and 7-9 months, respectively, for standard platinum-doublet chemotherapy regimens in patients with advanced NSCLC (12,13), the combination of S-1 with CDDP appears to be encouraging. In the present study, combination chemotherapy with S-1 (80 mg/m^2/day, days 1-21) and CDDP (60 mg/m^2 on day 8, every 5 weeks) yielded a potentially longer MST (17.9 months) than that for the abovementioned studies, despite the relatively low RR (17.5%). The modest improvement in survival observed in this study as compared with previous studies may be affected by various factors including the high rate of SD (62.5%), which extended the disease control rate to 80.0%, or the exclusion of patients with a performance status of 2. In addition, second- and/or third-line chemotherapy treatments may prolong the survival of patients with advanced NSCLC, as previously reported (14,15). In this study, 37 patients (92.5%) received second-line chemotherapy, involving platinum-based doublet chemotherapy, non-platinum-doublet chemotherapy, single